
MULTI-VIEW CAUSAL DISCOVERY WITHOUT NON-GAUSSIANITY: IDENTIFIABILITY AND ALGORITHMS

Anonymous authors

Paper under double-blind review

ABSTRACT

Causal discovery is a difficult problem that typically relies on strong assumptions on the data-generating model, such as non-Gaussianity. In practice, many modern applications provide multiple related views of the same system, which has rarely been considered for causal discovery. Here, we leverage this multi-view structure to achieve causal discovery with weak assumptions. We propose a multi-view linear Structural Equation Model (SEM) that extends the well-known framework of non-Gaussian disturbances by alternatively leveraging correlation over views. We prove the identifiability of the model for acyclic SEMs. Subsequently, we propose several multi-view causal discovery algorithms, inspired by single-view algorithms (DirectLiNGAM, PairwiseLiNGAM, and ICA-LiNGAM). The new methods are validated through simulations and applications on neuroimaging data, where they enable the estimation of causal graphs between brain regions.

1 INTRODUCTION

Causal discovery is a fundamental problem in scientific data analysis as well as several technological applications (Peters et al., 2017). The basic problem is that we are given a number of observed variables, and we need to infer which variables cause which, and with what “connection strengths”. In the typical case, we only observe the data passively without any possibility of performing interventions, and this purely observational quality of the data makes the problem difficult.

Often, the problem is formalized as a structural equation model (SEM) (Bollen, 1989), also called a functional causal model (Pearl, 2009). Then the question is how to estimate the SEM parameters using statistical theory. In fact, before even considering estimation methods, we need to know if it is at all possible to solve the problem. This is the question of *identifiability* of the model: can the parameters that describe the causal relations and directions be (uniquely) estimated?

A well-known fact is that if all variables are Gaussian and the model is linear, identifiability of the SEM is very problematic. Some of the earliest work showed that the directions can sometimes be recovered by an analysis of the *conditional independencies* between variables (Spirtes et al., 2001); however, this is only possible in some special cases and notably not possible when observing only two variables. Recent literature has, therefore, focused on different departures from the linear-Gaussian framework to achieve identifiability. A major advance was to consider a linear model together with *non-Gaussianity* (Shimizu et al., 2006), which leads to full identifiability of the model under weak conditions such as acyclicity; however, such non-Gaussianity may not be strong enough in many data sets. A related framework was proposed by assuming that the cause undergoes a *non-linear transform*, while the disturbance is still additive (Hoyer et al., 2008); however the nonlinearity may not be strong enough in many applications, and such nonlinearity slightly contradicts the linear additivity of the disturbance. Further related frameworks were proposed by (Peters & Bühlmann, 2014; Zhang & Hyvärinen, 2009; Monti et al., 2019). Each framework has led to development of a number of algorithms, the discussion of which we defer to the Background Section below.

An alternative recent framework is given by the *multi-view* setting, where data is collected from different sources whose similarities can be leveraged for estimation and identifiability. However, current approaches using multi-view structure are scarce and limited; either they assume the views are statistically independent (Shimizu, 2012) or make strong assumptions on their dependencies (Chen et al., 2024). Here, we consider the linear multi-view SEM, providing a general theory and algorithms that leverage that multi-view structure.

054 Our main contributions are:

- 055 1. We generalize some of the most well-known *algorithms* for single-view causal discovery
056 to the multi-view setting. The generalizations of PairwiseLiNGAM and DirectLiNGAM
057 result in completely new and fast causal discovery using second-order statistics only, while
058 our adaptation of ICA-LiNGAM improves on Chen et al. (2024).
059
- 060 2. We show that our algorithms are *consistent* under weak conditions: we can replace the
061 non-Gaussianity assumption on the disturbances by conditions on correlations between the
062 views and “diversity” of such second-order statistics (SOS). Still, if the disturbances are
063 non-Gaussian, we generalize Shimizu (2012); Chen et al. (2024).
064
- 065 3. The proofs above directly lead to rigorous *identifiability* results on the model, including
066 cases where all the disturbances are Gaussian, or, equivalently, identifiability results based
067 on SOS only. Importantly, only weak conditions on SOS is necessary for identifiability,
068 greatly generalizing previous work.
- 069 4. We make our algorithms usable by practitioners by providing them as *open-source*, and
070 demonstrate their usefulness by benchmarking them on real neuroimaging data.

071 2 BACKGROUND

072 **Causal ordering** In the following, we consider a random vector $\boldsymbol{x} \in \mathbb{R}^p$ whose entries are nodes of
073 a directed acyclic graph (DAG). The DAG is represented by an adjacency matrix $\boldsymbol{B} \in \mathbb{R}^{p \times p}$, where
074 non-zero values indicate the edges of the graph. The entries of \boldsymbol{x} can be reordered such that each
075 “causes” the next. This is formalized by the adjacency matrix admitting a special decomposition
076 $\boldsymbol{B} = \boldsymbol{P}^\top \boldsymbol{T} \boldsymbol{P}$, where \boldsymbol{T} is a strictly lower triangular matrix and \boldsymbol{P} is a permutation matrix referred
077 to as the *causal ordering*. In general, the causal ordering is not unique.

080 **LiNGAM: A single-view model for causal discovery** We consider a structural equation model
081 (SEM), also known as a functional causal model (Bollen, 1989; Pearl, 2009), that is linear and where
082 the data follows

$$083 \boldsymbol{x} = \boldsymbol{B}\boldsymbol{x} + \boldsymbol{e} \tag{1}$$

084 and the entries e_1, \dots, e_p of the random vector $\boldsymbol{e} \in \mathbb{R}^p$ are independent noise terms, or *disturbances*.
085 Causal discovery consists in inferring the parameters \boldsymbol{B} of the model, from observations of \boldsymbol{x} . Yet,
086 the identifiability of the model and therefore the uniqueness of \boldsymbol{B} is not straightforward. In fact, it is
087 well-known that with Gaussian disturbances, the model is unidentifiable in general (Richardson &
088 Spirtes, 2002; Genin, 2021). A major advance by Shimizu et al. (2006) was assuming *non-Gaussian*
089 disturbances, leading to their Linear Non-Gaussian Acyclic Model (LiNGAM).
090

091 **Identifiability of LiNGAM** Shimizu et al. (2006) showed that the LiNGAM model is identifiable
092 in terms of the matrix \boldsymbol{B} . A rigorous re-statement of this result is given in Appendix A.2. A further
093 question that has received less attention is under what conditions the model is identifiable in terms
094 of the causal ordering \boldsymbol{P} . In fact, it is not in general: specifically, there may exist many permutation
095 matrices \boldsymbol{P} and strictly lower triangular matrices \boldsymbol{T} such that the generated data has the same dis-
096 tribution and the generating permutation cannot be identified. For instance, in the degenerate case
097 $\boldsymbol{B} = \boldsymbol{T} = \mathbf{0}$, any permutation matrix \boldsymbol{P} is equally valid and gives the same data distribution; any
098 very sparse \boldsymbol{B} leads to several equally valid orderings. As is well-known, a DAG in general defines
099 only a *partial* ordering in the sense that for some pairs of variables, we cannot necessarily say which
100 is “earlier” and which is “later”. Thus, if we want to make the causal ordering unique — *i.e.* to
101 obtain a *total* ordering — we need further assumptions, as considered in later sections.

102 **Estimation of LiNGAM** Since the LiNGAM model was proposed, two important categories of
103 algorithms for estimating this model have been developed. First, algorithms based on *recursively*
104 computing the *residuals* of pairwise regressions include DirectLiNGAM (Shimizu et al., 2011) and
105 PairwiseLiNGAM (Hyvärinen & Smith, 2013). These compare pairs of variables from \boldsymbol{x} and deduce
106 what is the causal direction between the two variables based on regressing the variables in the two
107 directions. By aggregating this information, they finally determine a causal ordering \boldsymbol{P} . Once an

ordering is found, the matrix T can easily be obtained with conventional methods such as least-squares (LS) regression, which then gives $B = P^\top T P$.

The second category is the ICA-based algorithm that was proposed in the original LiNGAM paper (Shimizu et al., 2005). It is based on the observation that LiNGAM model can be rewritten as a latent variable model, in particular an ICA model (Hyvärinen et al., 2001) as

$$\mathbf{x} = \mathbf{A} \mathbf{s} . \tag{2}$$

Again, the entries in \mathbf{s} are independent and non-Gaussian, and the “mixing” matrix \mathbf{A} expresses how the data is generated from the latent variables \mathbf{s} . Many methods developed for ICA can be used to estimate the matrix \mathbf{A} . However, it is important to consider the special structure of the mixing, since $\mathbf{A} = (\mathbf{I} - \mathbf{B})^{-1}$, where \mathbf{B} is a DAG (Shimizu et al., 2006). This method first recovers the adjacency matrix \mathbf{B} , and then estimates a causal ordering P from \mathbf{B} .

3 A MULTI-VIEW MODEL FOR CAUSAL DISCOVERY

We now extend the linear acyclic model in Eq. 1 to the multi-view setting, leading to a Linear Multi-View Acyclic Model (LiMVAM). Suppose we observe m different views of a p -dimensional vector \mathbf{x}^i . The most general linear acyclic extension is

$$\mathbf{x}^i = \mathbf{B}^i \mathbf{x}^i + \mathbf{e}^i \tag{3}$$

for views $i \in \llbracket 1, m \rrbracket$. The \mathbf{B}^i are adjacency matrices of DAGs, and \mathbf{e}^i are view-specific disturbance vectors (with entries of non-zero variance). Similarly to Eq. 2, the LiMVAM model can equivalently be written as a latent-variable model

$$\mathbf{x}^i = \mathbf{A}^i \mathbf{e}^i \tag{4}$$

where the mixing matrix has a special structure, $\mathbf{A}^i = (\mathbf{I} - \mathbf{B}^i)^{-1}$, which we will exploit later in Section 5. Our model generalizes that by Chen et al. (2024), who assumed a specific structure on the influences, as will also be explained in Section 5.

To exploit the multi-view structure, we follow Shimizu (2012); Chen et al. (2024) and assume that all adjacency matrices \mathbf{B}^i share the same causal ordering. Equivalently, they admit a decomposition $\mathbf{B}^i = \mathbf{P}^\top \mathbf{T}^i \mathbf{P}$ where \mathbf{T}^i is strictly lower triangular and \mathbf{P} is a permutation matrix that is shared among the views i . Moreover, as commonly assumed in causal discovery, we require the components of each \mathbf{e}^i to be mutually independent, for any given i . (In contrast, correlations between views i and i' will be seen to be essential for identifiability.) Contrary to most existing approaches, we do not impose any restriction on the distribution of the disturbances, such as non-Gaussianity, which greatly broadens the applicability of the model.

The next two sections develop efficient methods for estimating the adjacency matrices \mathbf{B}^i , together with identifiability theory. We begin in Section 4 with methods that estimate the causal ordering using recursive residuals and using only second-order statistics, based on the single-view algorithms DirectLiNGAM (Shimizu et al., 2011) and PairwiseLiNGAM (Hyvärinen & Smith, 2013). Then, we propose a modified version of the ICA-based multi-view model from Chen et al. (2024) in Section 5.

4 ESTIMATION BY SOS AND RECURSIVE RESIDUALS

First, we show how to estimate the model using Second-Order Statistics (SOS) only, and how the SOS alone lead to identifiability. To do so, we will rely on a principle that we call *recursive residuals*. While it has been used by Shimizu et al. (2011); Hyvärinen & Smith (2013); Shimizu (2012), we provide here a unified treatment.

4.1 CAUSAL ORDERING USING RECURSIVE RESIDUALS

Methods based on what we call recursive residuals are built on the following principle: 1) we can find a root variable (*i.e.* one with no parents) by analyzing the causal directions between all the pairs of variables, and 2) when all other variables are regressed on a root variable, the resulting residuals preserve the causal ordering of the original variables (Shimizu et al., 2011, Lemma 2 and

Corollary 1). In the multi-view case, the same principles apply since all views are assumed to share a common ordering. A formal proof is provided in Appendix D.3.1 and D.3.2.

Algorithms based on recursive residuals therefore follow the same recursive scheme to recover the causal ordering: (i) perform pairwise regressions to obtain residuals, (ii) identify a root variable according to a specific criterion of causal direction computed on the residuals, and (iii) remove the selected root and repeat the procedure on the residuals until all variables are ordered. The main difference between algorithms lies in step (ii), *i.e.* in how the root variable is selected.

Since a root variable has no parents, we can find one by testing the causal direction for every pair of variables and taking as a root a variable that is never inferred to be an effect. A practical way to find the root variable from such tests with a finite sample is described in Appendix E.4.

Thus, root selection reduces to designing a criterion of causal direction capable of reliably distinguishing the causal direction between two variables. In the following, we introduce two new such criteria in the multi-view setting. For simplicity of notation, we consider two random variables aggregated across views: $\mathbf{x}_1 = (x_1^1, \dots, x_1^m)^\top$ and $\mathbf{x}_2 = (x_2^1, \dots, x_2^m)^\top$; either \mathbf{x}_1 causes \mathbf{x}_2 , or the converse. Covariance matrices are denoted by $\Sigma_{\mathbf{x}_1} = \mathbb{E}[\mathbf{x}_1 \mathbf{x}_1^\top]$, and likewise for \mathbf{x}_2 , e_1 and e_2 .

4.2 LIKELIHOOD-BASED CRITERION: PAIRWISELIMVAM

We first derive a criterion that extends the PairwiseLiNGAM criterion of Hyvärinen & Smith (2013) to the multi-view setting. Assuming Gaussian disturbances, we compute the expected log-likelihoods of two models: $\mathbf{x}_1 \rightarrow \mathbf{x}_2$ and $\mathbf{x}_2 \rightarrow \mathbf{x}_1$ (where an arrow denotes a directed edge between two adjacent variables in the causal graph). This leads to the following criterion, which is the logarithm of the maximum likelihood ratio (LR) between the two models:

$$\text{LR}_{12} = -\log \det \Sigma_{\mathbf{x}_1} - \log \det \Sigma_{e_2} + \log \det \Sigma_{\mathbf{x}_2} + \log \det \Sigma_{e_1} . \quad (5)$$

We prove in Appendix B that, under very weak constraints on the correlations of variables and views, this criterion is positive when $\mathbf{x}_1 \rightarrow \mathbf{x}_2$, and negative in the opposite direction, *no matter whether the disturbances are Gaussian or non-Gaussian*. Importantly, this makes the causal direction — and thus the entire causal ordering — identifiable under very general circumstances. So, although we developed this criterion for Gaussian disturbances, we emphasize that the resulting method is consistent regardless of the Gaussianity of the disturbances.

The necessary and sufficient conditions for the consistency of this criterion are given in Appendix B.6; a sufficient condition, assuming for simplicity that \mathbf{x}_1 is the cause, is that two views i, i' exist such that $|\text{corr}(e_2^i, e_2^{i'})| \neq |\text{corr}(x_1^i, x_1^{i'})|$, while $\text{corr}(x_1^i, e_2^i) \neq 0$ or $\text{corr}(x_1^{i'}, e_2^{i'}) \neq 0$. This essentially says that the views need to be correlated and the correlations need to be diverse, and will be explained in more detail below. In practice, we replace the covariance matrices $\Sigma_{\mathbf{x}_1}$, Σ_{e_1} , $\Sigma_{\mathbf{x}_2}$, and Σ_{e_2} with consistent estimators (see Appendix E.1); we use Ordinary LS to compute the residuals throughout this paper. Thus, we obtain a consistent estimator of the true direction.

4.3 CROSS-COVARIANCE-BASED CRITERION: DIRECTLIMVAM

Our next criterion is a new multi-view extension of the DirectLiNGAM criterion (Shimizu et al., 2011). In a single-view setting, Shimizu et al. (2011) relied on the fact that x_1 and e_2 are *independent* if the causal direction is $x_1 \rightarrow x_2$, and measured the independence using a kernel-based estimator of mutual information called KGV (Bach & Jordan, 2002). A multi-view extension was actually proposed by Shimizu (2012), where the correct direction was chosen by comparing the *sums over views* of these scores for the two directions. However, such summation over views does not fully take advantage of the multi-view structure. Thus, the disturbances still needed to be non-Gaussian.

Here, we efficiently exploit the multi-view framework while only looking at SOS. We choose to evaluate the *cross-covariance* between the *entire* vectors $\mathbf{x}_1 = (x_1^1, \dots, x_1^m)^\top$ and $\mathbf{e}_2 = (e_2^1, \dots, e_2^m)^\top$ for the direction $\mathbf{x}_1 \rightarrow \mathbf{x}_2$, and between \mathbf{x}_2 and \mathbf{e}_1 for the direction $\mathbf{x}_2 \rightarrow \mathbf{x}_1$. Specifically, the correct direction is chosen by comparing the Frobenius norms of the cross-covariances between regressors and residuals. Thus, we obtain the following criterion:

$$\text{FC}_{12} = \left\| \mathbb{E}[\mathbf{x}_2 \mathbf{e}_1^\top] \right\|_F - \left\| \mathbb{E}[\mathbf{x}_1 \mathbf{e}_2^\top] \right\|_F . \quad (6)$$

We prove in Appendix C that this criterion consistently finds the correct direction under the same conditions as the likelihood-based criterion, again *no matter whether the disturbances are Gaussian or non-Gaussian*.

4.4 ESTIMATING THE CAUSAL COEFFICIENTS

Applying the recursive scheme explained in Section 4.1, and using the criteria from Eq. 5 or Eq. 6, we obtain a causal ordering encoded by \mathbf{P} . Importantly, since the ordering is now known, the causal matrices \mathbf{B}^i can be uniquely recovered with little effort. In fact, the model becomes

$$\mathbf{x}^{i'} = \mathbf{T}^i \mathbf{x}^{i'} + \mathbf{e}^{i'}, \quad i \in [1, m] \quad (7)$$

where $\mathbf{x}^{i'} = \mathbf{P}\mathbf{x}^i$ are the reordered observations and $\mathbf{e}^{i'} = \mathbf{P}\mathbf{e}^i$ are the reordered disturbances. By construction, each variable $x_j^{i'}$ only depends on its predecessors $x_1^{i'}, \dots, x_{j-1}^{i'}$. For each $j \in [2, p]$, we estimate the j -th row of all matrices \mathbf{T}^i jointly using one-step Feasible Generalized Least Squares (FGLS) Zellner (1962), which is more efficient than Ordinary LS. A detailed description of one-step FGLS is provided in Appendix E.5. Under the assumption that disturbances are mutually independent within each view, FGLS yields a unique regression for every variable on its parents. Finally, the adjacency matrices are recovered as $\mathbf{B}^i = \mathbf{P}^\top \mathbf{T}^i \mathbf{P}$.

The overall procedure is summarized in Algorithm 3 in the Appendix; it notably requires no hyperparameter tuning. Its worst-case *computational complexity* is in $O(m^3 \cdot p^3 \cdot n)$, which we show in Appendix E.7. In practice, these algorithms are highly parallelizable as they rely on basic algebraic operations (e.g. multiplying pairs of matrices), and fast as they do not require numerical optimization of an objective function.

4.5 IDENTIFIABILITY USING SECOND-ORDER STATISTICS

We can build an identifiability theory based on the conditions required by the criteria LR and FC (given in Appendices B and C). We start by formulating the following central assumption, which will be seen to be a sufficient condition for identifiability. Even milder sufficient conditions are discussed in Appendix D.1 but they are harder to interpret.

Assumption 1 (Correlation and diversity across views) *For any two variables \mathbf{x}_j and $\mathbf{x}_{j'}$ such that $\mathbf{x}_j \rightarrow \mathbf{x}_{j'}$ (in the sense that $\mathbf{B}_{j',j}^i \neq 0$ for at least one i), there exist two distinct views $i \neq i'$ such that a) those variables are correlated in at least one of those views, $\text{corr}(x_j^i, x_{j'}^{i'}) \neq 0$ or $\text{corr}(x_j^{i'}, x_{j'}^i) \neq 0$, and b) their correlations fulfill the “diversity” condition:*

$$|\text{corr}(x_j^i, x_{j'}^{i'})| \neq |\text{corr}(e_{j'}^i, e_{j'}^{i'})| . \quad (8)$$

To better understand this assumption, note first that it requires some *correlation across views*: it rules out the trivial case where all cross-view correlations are zero. Moreover, it demands some *diversity* in these correlations. Consider the extreme situation where, for standardized variables, $x_j^i = \alpha x_{j'}^{i'}$ and $x_{j'}^{i'} = \alpha x_j^i$ (and analogously for the residuals), for some scalar α . In this case, all correlations equal 1, so condition Eq. 8 is violated. Appendix D.2 provides more realistic examples of violations. We next introduce an additional assumption that ensures identifiability of the total causal ordering.

Assumption 2 (Dense connectivity of the graph when pooled across views) *Let \mathcal{G} denote the union graph of the m views, obtained by taking the union of their edge sets, and assume that the ordering induced by \mathcal{G} is total, i.e. there exists a directed path between any two variables.*

With these assumptions, we prove in Appendix D.3 the following identifiability result.

Theorem 1 (Identifiability of the ordering and adjacency matrices \mathbf{B}^i) *Assume the data follows the model in Eq. 3, and that Assumption 1 holds. Then, causal (partial) ordering and causal coefficients \mathbf{B}^i are identifiable. If we further make Assumption 2, then \mathbf{P} is identifiable as well.*

The identifiability of the *partial* ordering does not necessarily mean that the permutation matrix \mathbf{P} can be recovered uniquely. If the ordering is only partial (for example, in a three-nodes graph: $\mathbf{x}_1 \rightarrow \mathbf{x}_2$ and $\mathbf{x}_1 \rightarrow \mathbf{x}_3$, but there is no relation between \mathbf{x}_2 and \mathbf{x}_3 , so both orderings $1 \rightarrow 2 \rightarrow 3$ and $1 \rightarrow 3 \rightarrow 2$ are valid), then \mathbf{P} is only identifiable up to a class of permutations that induce the same partial ordering. The above theorem shows a case where \mathbf{P} can be (uniquely) identified.

5 ESTIMATION BY NON-GAUSSIANITY ASSUMING SHARED DISTURBANCES

Next, we provide an alternative approach to the LiMVAM model definition and estimation. We utilize the non-Gaussianity of the disturbances to obtain identifiability conditions that are different from the previous section. However, we still do not impose non-Gaussianity as a necessary condition.

Model definition The approach here is to propose a particular model for the disturbances by supposing that they can be additively composed into two terms: one term is view-specific, while the other is shared across views and therefore makes the views dependent. Specifically:

Assumption 3 (Shared disturbances) *The disturbances can be decomposed as*

$$e^i = D^i s + n^i \quad (9)$$

where the D^i are diagonal matrices with positive entries on the diagonal, the s has mutually independent entries and second-order moment $\mathbb{E}[ss^\top] = I_p$, and the view-specific noises are Gaussian $n^i \sim \mathcal{N}(\mathbf{0}, \Sigma^i)$ and depend on the view i via the second-order moments Σ^i that are diagonal matrices. Lastly, the vectors s and $n^i, i = 1, \dots, m$, are assumed to be mutually independent.

This Assumption and Eq. 9 are related to Chen et al. (2024) who were originally inspired by the multi-view Shared ICA of Richard et al. (2021). Specifically, Chen et al. (2024) considered the special case where the matrices $D^i = I_p$, so that there are the same disturbances s over views. We argue here that their model was too restrictive and unrealistic as it imposes an arbitrary scaling for the data variables. Consider the root variable of the DAG, denoting it by x_i . Its disturbance is $s_i + n_i$ which has variance of at least one since the variance of s_i is defined as one. Thus, the root variable has variance of at least one which is absurd: the model should be invariant to the scaling of the variables. Likewise, suppose we create a new data set by dividing just one view, say x^1 by, say 10, giving new data x'^1 . This new data does not follow the model by Chen et al. (2024) anymore since s should be rescaled to $s/10$ for just this view; now the $s/10$ here is different from the s in other views. Such problems motivated us to develop a model where the scaling terms D^i are new parameters, and thus to the definition in Eq. 9.

Identifiability Now we proceed to show the identifiability of the model based on Assumption 3. The starting point is that our model can be rewritten as a multi-view ICA model as in Eq. 4, just like in the case of LiNGAM. Thus, the methods developed for multi-view ICA can be used to analyze its identifiability. We first discuss the assumptions used for our theorems.

Assumption 4 (Diversity of the views with Gaussian disturbances) *If j and j' , $j \neq j'$, are the indices of two Gaussian common disturbances in s , then the number of views is at least three, and there exists a view i such that $\frac{\Sigma_{jj}^i}{(D_{jj}^i)^2} \neq \frac{\Sigma_{j'j'}^i}{(D_{j'j'}^i)^2}$.*

This assumption, inspired by Richard et al. (2021), is trivially fulfilled if all disturbances are non-Gaussian. For Gaussian disturbances, it essentially states that the views should be diverse in terms of disturbances' SOS. This follows from the theory of Shared ICA which does not require the common disturbances s to be non-Gaussian if there is enough diversity (Richard et al., 2021; Anderson et al., 2013). The next assumption assumes that the union graph of the B^i is dense enough across views.

Assumption 5 (Dense connectivity of the graph when pooled across views) *There exists a permutation \bar{P} such that the matrices $\bar{T}^i = \bar{P}B^i\bar{P}^\top$ are strictly lower triangular, and for each entry (j, k) with $j > k$, there is at least one view i such that $\bar{T}_{j,k}^i \neq 0$.*

Note that this assumption is quite weak as the T^i can be very sparse. This is especially the case when the number of views is large, since only one non-zero entry is required over all views.

We can now state our main identifiability result for this variant of the model.

Theorem 2 (Identifiability with shared disturbances) *Assume the LiMVAM model in Eq. 3 together with Assumption 3. Under Assumption 4, the model is identifiable in the sense that the parameters B^i , D^i , and Σ^i are identifiable. If we further make Assumption 5, P is identifiable as well.*

The proof of the theorem is given in Appendix F. We thus see that for non-Gaussian disturbances, identifiability is achieved with weak conditions; in fact, no special conditions on the covariances are

324
325
326
327
328
329
330
331
332
333
334
335
336
337
338
339
340
341
342
343
344
345
346
347
348
349
350
351
352
353
354
355
356
357
358
359
360
361
362
363
364
365
366
367
368
369
370
371
372
373
374
375
376
377

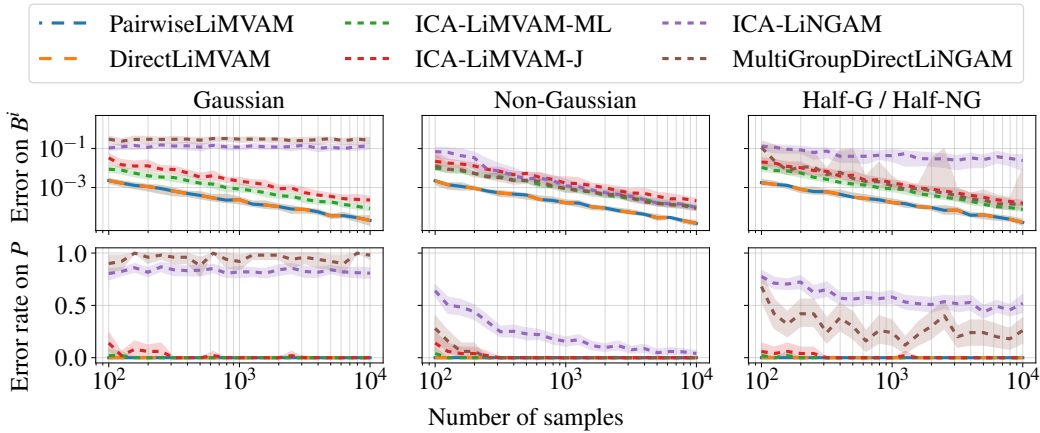


Figure 1: Separation performance of three recursive residuals algorithms and three ICA-based algorithms. We assume shared disturbances as in Eq. 9. We used 50 different seeds. Lower is better.

needed. Still, the theory of Shared ICA leads to identifiability even for Gaussian disturbances, but with stronger conditions than obtained in Section 4. The utility of the Shared ICA theory lies also in the fact that it allows us to construct an algorithm very easily.

Estimation The model can be estimated by a combination of the ICA-based estimation procedure by Shimizu et al. (2006), combined with the Shared ICA methods by Richard et al. (2021). We call it ICA-LiMVAM and explain it in detail in Algorithm 4. Surprisingly, the resulting algorithm gives estimates of B_i that are identical to Chen et al. (2024), even though our model is more general. In contrast, our algorithm estimates different noise variances and scalings D_i . The worst-case *computational complexity* is in $O(tnmp^3 + mp^5)$, for t iterations of the Shared ICA (ML) algorithm, n samples, m views and p components. We detail this in Appendix G.2.

6 EXPERIMENTS

6.1 SIMULATIONS

We benchmark a total of six multi-view causal discovery algorithms on synthetic data. Three of these algorithms are based on recursive residuals: our PairwiseLiMVAM and DirectLiMVAM, as well as MultiGroupDirectLiNGAM from Shimizu (2012). The other three algorithms are ICA-based: ICA-LiMVAM which is essentially the same as Chen et al. (2024), as well as ICA-LiNGAM (Shimizu et al., 2006) which is naively applied to each view, separately. Note that ICA-LiMVAM comes in two variants, each using a different Shared ICA algorithm: either Shared ICA “ML”, a likelihood-based method that can handle both Gaussian and non-Gaussian disturbances, or Shared ICA “J”, which jointly diagonalizes covariance matrices without using non-Gaussianity.

The first synthetic experiment is inspired by Richard et al. (2021). We monitor the performance of causal discovery algorithms across varying sample sizes and disturbance distributions. More specifically, the data are generated according to the LiMVAM model with shared disturbances from Eq. 9. The performance of the causal discovery algorithms is measured by the ℓ_2 distance between true and

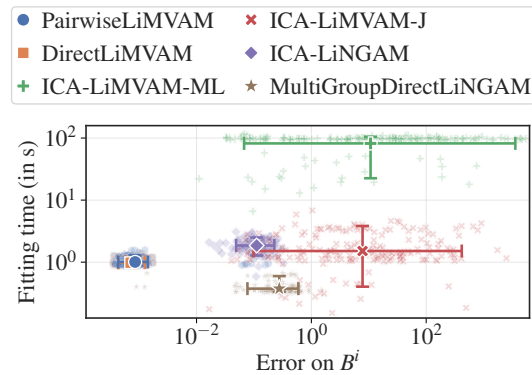


Figure 2: Estimation error of the adjacency matrices B^i versus total fitting time for each method, across 200 random runs with $m = 6$ views, $p = 5$ variables, and $n = 1000$ samples. Disturbances are drawn from a standard Gaussian. Note that the point clouds for PairwiseLiMVAM and DirectLiMVAM largely overlap.

378 estimated adjacency matrices B^i , and the percentage of incorrectly estimated causal orders P over
 379 50 random runs.

380 Results of the first synthetic experiment are plotted in Figure 1. Our algorithms PairwiseLiMVAM
 381 and DirectLiMVAM consistently outperform all others by a significant margin. ICA-LiMVAM
 382 yields reliable estimates but with larger errors. In contrast, MultiGroupDirectLiNGAM and ICA-
 383 LiNGAM, which are designed for non-Gaussian disturbances, fail entirely in the Gaussian setting,
 384 as expected. Note that the high error rate of ICA-LiNGAM in recovering the causal ordering P is
 385 likely explained by its inability to exploit that the ordering is shared across views.
 386

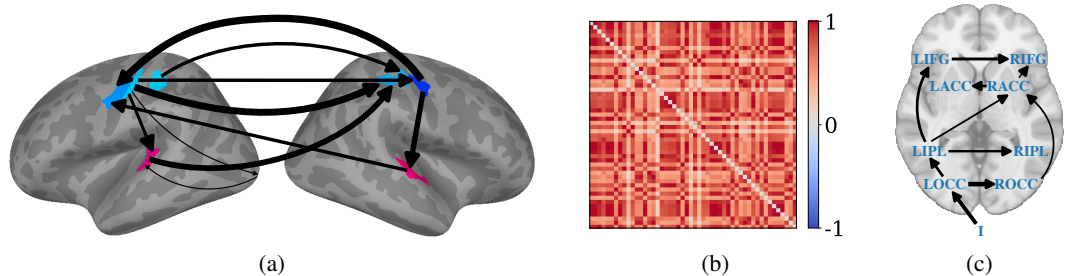
387 For the second synthetic experiment, we report the trade-off between computational complexity and
 388 estimation error of the adjacency matrices. We use a different data generation model, described
 389 by Eq. 3 where the disturbances are Gaussian with equal variances. This breaks the assumptions for
 390 all methods but our PairwiseLiMVAM and DirectLiMVAM. As expected, we see in Figure 2 that our
 391 algorithms PairwiseLiMVAM and DirectLiMVAM provide a major reduction in estimation errors,
 392 at little or no computational cost. In contrast, the four other algorithms struggle with this data.

393 In Appendix H, we include further experiments that test Assumptions 4 and 5, as well as scalability
 394 with more views and variables. In particular, we find that DirectLiMVAM outperforms Pairwise-
 395 LiMVAM in some cases, which is less obvious from Figures 1 and 2 alone.

396 6.2 REAL DATA EXPERIMENTS WITH MEG

397 Next, we performed experiments on magnetoencephalography (MEG) data measuring human brain
 398 activity. MEG data has a high temporal resolution, so typically methods related to Granger causality
 399 are used. However, we are here interested in analyzing the *energies of oscillatory* signals. The
 400 energies change very slowly (on the time-scale of seconds), while the underlying brain activity
 401 being measured is likely to change much more quickly. Thus, it is appropriate to use a model of
 402 instantaneous causality as in our model.
 403

404 We used the Cam-CAN dataset, which is the largest publicly available MEG dataset (Shafto et al.,
 405 2014; Taylor et al., 2017), and considered the “sensorimotor task” during which each participant
 406 had to respond with a right index finger button press to auditory/visual stimuli. Further details are
 407 available in Appendix H.2.1. We applied PairwiseLiMVAM to these data, each of the 98 participants
 408 being one view. The experiment ran in 2 hours and 20 minutes using 5 CPUs. Although our model
 409 does not require or assume any similarity across the matrices T^i , one may reasonably hypothesize
 410 that the participants’ brains share structural patterns. So, to facilitate population-level interpretation,
 411 we computed the element-wise median of the B^i matrices.
 412



422 Figure 3: (a) Top ten strongest median causal effects (estimated by PairwiseLiMVAM) across 98
 423 Cam-CAN (MEG) participants. (b) Pearson correlations between median causal matrices across
 424 50 runs in MEG. (c) Top ten strongest median causal effects from PairwiseLiMVAM across 9 fMRI
 425 participants. Arrows indicate direction and strength of effects, with width proportional to magnitude.
 426

427 Fig. 3a displays the ten strongest (in absolute value) median causal effects. Notably, many causal
 428 connections are between homologous regions across hemispheres — particularly within the primary
 429 motor and somatosensory cortices — consistent with prior findings that symmetric brain regions
 430 exhibit strong inter-hemispheric correlations Li et al. (1996). Additionally, numerous arrows involve
 431 the postcentral regions, which have been implicated in fine motor control and hand-related tasks
 Braun et al. (2002). To evaluate the robustness of the results, we repeated the experiment 50 times,

each time randomly selecting 30 participants from the full cohort. We assessed consistency by measuring the Pearson correlation between the resulting median matrices across runs. As shown in Figure 3b, the median effects are highly correlated across different subsets (average correlation: 0.67), demonstrating the stability of our method. Additional experiments using ICA-LiMVAM-ML are reported in Appendix H.2.2.

6.3 REAL DATA EXPERIMENTS WITH FMRI

We also evaluated PairwiseLiMVAM on an fMRI rhyming judgment task dataset (Ramsey et al., 2010). The data consist of recordings from nine participants, each represented by nine variables: one task regressor (Input I), obtained by convolving the boxcar design of the rhyming task with a canonical hemodynamic response function, and eight regional time series from bilateral regions of interest. The dataset was acquired on a 3T scanner with a repetition time of 2 s, yielding 160 samples per subject, and is available via the OpenfMRI project (preprocessed version from ¹).

We report the ten strongest effects from the element-wise median of the estimated adjacency matrices in Figure 3c. The recovered structure is consistent with established findings for this task. In particular, we find a strong edge from the task regressor to the left occipital cortex (Input \rightarrow LOCC), reflecting the expected visual drive of the stimuli, and prominent connections from left to right homologous regions (*e.g.* LOCC \rightarrow ROCC, LIFG \rightarrow RIFG, LIPL \rightarrow RIPL), in line with the left-hemisphere dominance and inter-hemispheric influences reported by Ramsey et al. (2010). Edges such as LOCC \rightarrow LACC and connections between LACC and RACC also match relationships highlighted in their analyses.

7 DISCUSSION AND RELATED WORK

A multi-view causal model based on LiNGAM was considered by Shimizu (2012), but their model was very different. The fundamental difference is that we assume the disturbances have some shared information across views and can be Gaussian, whereas Shimizu (2012) estimates disturbances that are independent across views and necessarily non-Gaussian. Thus, they only showed how to use the multiple views to improve the estimation while still assuming non-Gaussianity of the disturbances.

Chen et al. (2024) considered multi-view SEM using a special case of our shared disturbances model, which is in its turn a special case of our general LiMVAM model. Algorithmically, there is little difference between their work and our ICA-LiMVAM. However, their identifiability proofs are not available nor did they consider the identifiability of the causal ordering, while we do both. Moreover, as we already argued in Section 5, their model formulation has the serious flaw that it forces an arbitrary scaling of the data variables. Crucially, we propose new algorithms, PairwiseLiMVAM and DirectLiMVAM, that use only SOS; they are shown to be empirically superior to the ICA-LiMVAM in most cases.

A related very general framework, allowing for various kinds of interventions, was proposed by Mooij et al. (2020). On the other hand, a related “multi-context” approach, where the disturbances are not necessarily related at all while the DAGs are, was proposed by Sturma et al. (2023).

8 CONCLUSION

We propose a new approach for causal discovery in the multi-view linear-DAG case, improving the earlier work by Shimizu (2012); Chen et al. (2024). We show that the model is fully identifiable by second-order statistics (covariance structure) only, and under much weaker conditions than by Chen et al. (2024). We develop algorithms that either use the SOS only or combine them with non-Gaussian statistics. In particular, we adapt the Pairwise and Direct approaches to the multi-view case, resulting in highly efficient estimation. Results on brain imaging data are promising.

¹<https://github.com/cabal-cmu/Feedback-Discovery>

486
487
488
489
490
491
492
493
494
495
496
497
498
499
500
501
502
503
504
505
506
507
508
509
510
511
512
513
514
515
516
517
518
519
520
521
522
523
524
525
526
527
528
529
530
531
532
533
534
535
536
537
538
539

REFERENCES

- Jeffrey Adams, Niels Hansen, and Kun Zhang. Identification of partially observed linear causal models: Graphical conditions for the non-gaussian and heterogeneous cases. *Advances in Neural Information Processing Systems*, 34:22822–22833, 2021.
- Matthew Anderson, Gengshen Fu, Ronald Phlypo, and Tulay Adali. Independent vector analysis: Identification conditions and performance bounds. *IEEE Transactions on Signal Processing*, 62: 4399–4410, 2013.
- Francis R Bach and Michael I Jordan. Kernel independent component analysis. *Journal of machine learning research*, 3(Jul):1–48, 2002.
- Kenneth A Bollen. *Structural equations with latent variables*, volume 210. John Wiley & Sons, 1989.
- Christoph Braun, Monika Haug, Katja Wiech, Niels Birbaumer, Thomas Elbert, and Larry E Roberts. Functional organization of primary somatosensory cortex depends on the focus of attention. *Neuroimage*, 17(3):1451–1458, 2002.
- Wei Chen, Xiaokai Huang, Zijian Li, Ruichu Cai, Zhiyi Huang, and Zhifeng Hao. Individual causal structure learning from population data. In *Proceedings of the Thirty-Third International Joint Conference on Artificial Intelligence*, pp. 7109–7117, 2024.
- Pierre Comon. Independent component analysis, a new concept? *Signal Processing*, 36(3):287–314, 1994. ISSN 0165-1684. Higher Order Statistics.
- Anders M Dale, Bruce Fischl, and Martin I Sereno. Cortical surface-based analysis: I. segmentation and surface reconstruction. *Neuroimage*, 9(2):179–194, 1999.
- Konstantin Genin. Statistical undecidability in linear, non-gaussian causal models in the presence of latent confounders. In M. Ranzato, A. Beygelzimer, Y. Dauphin, P.S. Liang, and J. Wortman Vaughan (eds.), *Advances in Neural Information Processing Systems*, volume 34, pp. 13564–13574. Curran Associates, Inc., 2021.
- AmirEmad Ghassami, Negar Kiyavash, Biwei Huang, and Kun Zhang. Multi-domain causal structure learning in linear systems. *Advances in neural information processing systems*, 31, 2018.
- Alexandre Gramfort, Martin Luessi, Eric Larson, Denis A. Engemann, Daniel Strohmeier, Christian Brodbeck, Roman Goj, Mainak Jas, Teon Brooks, Lauri Parkkonen, and Matti Hämäläinen. Meg and eeg data analysis with mne-python. *Frontiers in Neuroscience*, 7, 2013. ISSN 1662-453X.
- Alexandre Gramfort, Martin Luessi, Eric Larson, Denis A. Engemann, Daniel Strohmeier, Christian Brodbeck, Lauri Parkkonen, and Matti S. Hämäläinen. Mne software for processing meg and eeg data. *NeuroImage*, 86:446–460, 2014. ISSN 1053-8119.
- William H Greene. *Econometric analysis*. Pearson education india, 2003.
- M. S. Hämäläinen and R. J. Ilmoniemi. Interpreting magnetic fields of the brain: minimum norm estimates. *Medical & Biological Engineering & Computing*, 32(1):35–42, 1994.
- Patrik Hoyer, Dominik Janzing, Joris M Mooij, Jonas Peters, and Bernhard Schölkopf. Nonlinear causal discovery with additive noise models. *Advances in neural information processing systems*, 21, 2008.
- Aapo Hyvärinen and Stephen M. Smith. Pairwise likelihood ratios for estimation of non-Gaussian structural equation models. *Journal of Machine Learning Research*, 14:111–152, 2013.
- Aapo Hyvärinen, Juha Karhunen, and Erkki Oja. *Independent Component Analysis*. Wiley Inter-science, 2001.

-
- 540 Sheraz Khan, Javeria A. Hashmi, Fahimeh Mamashli, Konstantinos Michmizos, Manfred G.
541 Kitzbichler, Hari Bharadwaj, Yousra Bekhti, Santosh Ganesan, Keri-Lee A. Garel, Susan
542 Whitfield-Gabrieli, Randy L. Gollub, Jian Kong, Lucia M. Vaina, Kunjan D. Rana, Steven M.
543 Stufflebeam, Matti S. Hämäläinen, and Tal Kenet. Maturation trajectories of cortical resting-
544 state networks depend on the mediating frequency band. *NeuroImage*, 174:57–68, 2018. ISSN
545 1053-8119.
- 546 A Li, F Z Yetkin, R Cox, and V M Haughton. Ipsilateral hemisphere activation during motor and
547 sensory tasks. *American Journal of Neuroradiology*, 17(4):651–655, 1996. ISSN 0195-6108.
548
- 549 Ricardo Pio Monti, Kun Zhang, and Aapo Hyvärinen. Causal discovery with general non-linear
550 relationships using non-linear ICA. In *Proc. 35th Conf. on Uncertainty in Artificial Intelligence*
551 *(UAI2019)*, Tel Aviv, Israel, 2019.
552
- 553 Joris M Mooij, Sara Magliacane, and Tom Claassen. Joint causal inference from multiple contexts.
554 *Journal of machine learning research*, 21(99):1–108, 2020.
- 555 Judea Pearl. *Causality: Models, Reasoning and Inference*. Cambridge University Press, USA, 2nd
556 edition, 2009. ISBN 052189560X.
557
- 558 Ronan Perry, Julius Von Kügelgen, and Bernhard Schölkopf. Causal discovery in heterogeneous
559 environments under the sparse mechanism shift hypothesis. *Advances in Neural Information*
560 *Processing Systems*, 35:10904–10917, 2022.
- 561 Jonas Peters and Peter Bühlmann. Identifiability of gaussian structural equation models with equal
562 error variances. *Biometrika*, 101(1):219–228, 2014.
563
- 564 Jonas Peters, Peter Bühlmann, and Nicolai Meinshausen. Causal inference by using invariant pre-
565 diction: identification and confidence intervals. *Journal of the Royal Statistical Society Series B:*
566 *Statistical Methodology*, 78(5):947–1012, 2016.
- 567 Jonas Peters, Dominik Janzing, and Bernhard Schölkopf. *Elements of causal inference: foundations*
568 *and learning algorithms*. The MIT Press, 2017.
569
- 570 Lindsey Power, Cédric Allain, Thomas Moreau, Alexandre Gramfort, and Timothy Bardouille. Us-
571 ing convolutional dictionary learning to detect task-related neuromagnetic transients and ageing
572 trends in a large open-access dataset. *NeuroImage*, 267:119809, 2023. ISSN 1053-8119.
573
- 574 Joseph D Ramsey, Stephen José Hanson, Catherine Hanson, Yaroslav O Halchenko, Russell A Pol-
575 drack, and Clark Glymour. Six problems for causal inference from fmri. *neuroimage*, 49(2):
576 1545–1558, 2010.
- 577 Hugo Richard, Pierre Ablin, Bertrand Thirion, Alexandre Gramfort, and Aapo Hyvarinen. Shared
578 independent component analysis for multi-subject neuroimaging. In *Advances in Neural Infor-*
579 *mation Processing Systems*, volume 34, pp. 29962–29971. Curran Associates, Inc., 2021.
580
- 581 Thomas Richardson and Peter Spirtes. Ancestral graph Markov models. *The Annals of Statistics*, 30
582 (4):962 – 1030, 2002.
- 583 Meredith A. Shafto, Lorraine K. Tyler, Marie Dixon, Jason R. Taylor, James Benedict Rowe, Rhodri
584 Cusack, Andrew J. Calder, William D. Marslen-Wilson, John S. Duncan, T. Dalgleish, Richard
585 N. A. Henson, Carol Brayne, and Fiona E. Matthews. The cambridge centre for ageing and
586 neuroscience (cam-can) study protocol: a cross-sectional, lifespan, multidisciplinary examination
587 of healthy cognitive ageing. *BMC Neurology*, 14, 2014.
- 588 Shohei Shimizu. Joint estimation of linear non-gaussian acyclic models. *Neurocomputing*, 81:
589 104–107, 2012.
590
- 591 Shōhei Shimizu. *Statistical Causal Discovery: LiNGAM Approach*. Springer, 2022.
592
- 593 Shohei Shimizu, Aapo Hyvärinen, Yutaka Kano, and Patrik O. Hoyer. Discovery of non-gaussian
linear causal models using ica. In *Conference on Uncertainty in Artificial Intelligence*, 2005.

594 Shohei Shimizu, Patrik O Hoyer, Aapo Hyvärinen, Antti Kerminen, and Michael Jordan. A linear
595 non-gaussian acyclic model for causal discovery. *Journal of Machine Learning Research*, 7(10),
596 2006.

597 Shohei Shimizu, Takanori Inazumi, Yasuhiro Sogawa, Aapo Hyvarinen, Yoshinobu Kawahara,
598 Takashi Washio, Patrik O Hoyer, Kenneth Bollen, and Patrik Hoyer. Directlingam: A direct
599 method for learning a linear non-gaussian structural equation model. *Journal of Machine Learn-*
600 *ing Research-JMLR*, 12(Apr):1225–1248, 2011.

601 Peter Spirtes, Clark Glymour, and Richard Scheines. *Causation, prediction, and search*. MIT press,
602 second edition edition, 2001.

603 Nils Sturma, Chandler Squires, Mathias Drton, and Caroline Uhler. Unpaired multi-domain causal
604 representation learning. In A. Oh, T. Naumann, A. Globerson, K. Saenko, M. Hardt, and S. Levine
605 (eds.), *Advances in Neural Information Processing Systems*, volume 36, pp. 34465–34492. Curran
606 Associates, Inc., 2023.

607 S Taulu and J Simola. Spatiotemporal signal space separation method for rejecting nearby interfer-
608 ence in meg measurements. *Physics in Medicine & Biology*, 51(7):1759, mar 2006.

609 Jason R. Taylor, Nitin Williams, Rhodri Cusack, Tibor Auer, Meredith A. Shafto, Marie Dixon,
610 Lorraine K. Tyler, Cam-CAN, and Richard N. Henson. The cambridge centre for ageing and
611 neuroscience (cam-can) data repository: Structural and functional mri, meg, and cognitive data
612 from a cross-sectional adult lifespan sample. *NeuroImage*, 144:262–269, 2017. ISSN 1053-8119.
613 Data Sharing Part II.

614 Arnold Zellner. An efficient method of estimating seemingly unrelated regressions and tests for
615 aggregation bias. *Journal of the American Statistical Association*, 57(298):348–368, 1962. doi:
616 10.2307/2281644.

617 Kun Zhang and Aapo Hyvärinen. On the identifiability of the post-nonlinear causal model. In *Proc.*
618 *25th Conference on Uncertainty in Artificial Intelligence (UAI2009)*, pp. 647–655, Montréal,
619 Canada, 2009.

620
621
622
623
624
625
626
627
628
629
630
631
632
633
634
635
636
637
638
639
640
641
642
643
644
645
646
647

648
649
650
651
652
653
654
655
656
657
658
659
660
661
662
663
664
665
666
667
668
669
670
671
672
673
674
675
676
677
678
679
680
681
682
683
684
685
686
687
688
689
690
691
692
693
694
695
696
697
698
699
700
701

APPENDIX

The appendix is organized as follows.

In Section A, we rigorously restate known identifiability results for LiNGAM.

In Section B, we prove the consistency of the likelihood-based criterion for a pair of variables.

In Section C, we prove the consistency of the cross-covariance-based criterion for a pair of variables.

In Section D, we extend the consistency of these criteria for a pair of variables to *many* pairs, and show that the LiMVAM model is identifiable.

In Section E, we show how to implement algorithms used to identify the causal graph.

In section F, we prove the identifiability of a special case of LiMVAM with shared disturbances.

In section G, we present an algorithm for estimating the causal graph in this special case.

In section H, we detail our experiments on real and synthetic data.

A	LiNGAM	15
A.1	Technical lemmas	15
A.2	Identifiability of LiNGAM	15
A.3	Proofs of technical lemmas	16
B	Likelihood-based criterion	18
B.1	Basic setting	18
B.2	Derivation of the expected log-likelihood in one direction	18
B.3	Derivation of the likelihood-based criterion	18
B.4	Non-negativity of the likelihood-based criterion	19
B.5	Proof of a useful lemma	20
B.6	Conditions for strict positivity of the likelihood-based criterion	21
C	Cross-covariance-based criterion	23
C.1	Derivation of the cross-covariance-based criterion	23
C.2	Conditions for strict positivity of the cross-covariance criterion	23
D	Identifiability of LiMVAM	24
D.1	Multivariate conditions for strict positivity of a criterion	24
D.2	An example for interpreting the SOS-based identifiability condition in Assumption 1	24
D.3	Proof of Theorem 1	26
E	SOS-based Algorithms for LiMVAM	28
E.1	Consistent estimator of the likelihood-based criterion	28
E.2	Consistent estimator of the cross-covariance-based criterion	28
E.3	Algorithms for estimating the two criteria	29
E.4	How to find the root variable	29
E.5	One-step Feasible Generalized Least Squares (FGLS)	30

702	E.6 Full algorithm	31
703		
704	E.7 Computational complexity	31
705		
706	F Identifiability of LiMVAM with shared disturbances	33
707		
708	F.1 Proof of Theorem 2 (first claim)	33
709	F.2 Proof of Theorem 2 (second claim)	33
710	F.3 Results for view-specific causal orderings	34
711		
712	G ICA-based Algorithm for LiMVAM with shared disturbances	35
713		
714	G.1 ICA-based Algorithm	35
715	G.2 Computational complexity	35
716		
717	H Experiments	37
718		
719	H.1 Synthetic experiments	37
720	H.2 Real data experiments	40
721		
722	I Distinction between multi-view and multi-domain frameworks	43
723		
724		
725		
726		
727		
728		
729		
730		
731		
732		
733		
734		
735		
736		
737		
738		
739		
740		
741		
742		
743		
744		
745		
746		
747		
748		
749		
750		
751		
752		
753		
754		
755		

756 A LINGAM

757
758 **Defining a domain connecting ICA and SEM parameters** In the following proofs, we define
759 the set

$$760 \mathcal{W} = \{\mathbf{W} \in \mathbb{R}^{p \times p} \mid \text{there exist a diagonal matrix } \mathbf{D} \text{ with positive diagonal entries} \quad (10)$$

$$761 \text{ and a DAG matrix } \mathbf{B}, \text{ such that } \mathbf{W} = \mathbf{D}^{-1}(\mathbf{I} - \mathbf{B})\}$$

762 as the domain of the “unmixing matrices” $\mathbf{W} = \mathbf{A}^{-1}$ in the ICA model from Eq. 2, that are
763 compatible with the DAG structure in the structural equation model (SEM) from Eq. 1. In general,
764 unmixing matrices are not constrained in the ICA model, except by invertibility (and possibly by
765 normalizing their rows). However, in the context of SEM estimation, the requirement that $\mathbf{W} =$
766 $\mathbf{D}^{-1}(\mathbf{I} - \mathbf{B})$ belongs to the set \mathcal{W} is a key structural constraint. Furthermore, it should be noted
767 that finding \mathbf{W} is equivalent to finding \mathbf{D} and \mathbf{B} , since they are related by $\mathbf{B} = \mathbf{D}^{-1}(\mathbf{I} - \mathbf{W})$.

768 Finally, we will use the fact that any DAG matrix \mathbf{B} can be decomposed into $\mathbf{B} = \mathbf{P}^\top \mathbf{T} \mathbf{P}$, where
769 \mathbf{P} is a permutation matrix and \mathbf{T} a strictly lower triangular matrix.

772 A.1 TECHNICAL LEMMAS

773 The following two lemmas are about matrices in the context of DAGs. They are used in the proofs
774 of Theorems 5, 2, and 8, and are proven in Appendix A.3.

775 The basic identifiability results for the causal matrices \mathbf{B}^i use the following:

776 **Lemma 3** *Let $\mathbf{W} = \mathbf{D}^{-1}(\mathbf{I} - \mathbf{B})$ and $\mathbf{W}' = \mathbf{D}'^{-1}(\mathbf{I} - \mathbf{B}')$ be two matrices that belong to \mathcal{W}
777 (defined in Eq. 10), and let \mathbf{Q} be a sign-permutation matrix. Then*

$$778 \mathbf{W}' = \mathbf{Q}^\top \mathbf{W} \implies \mathbf{Q} = \mathbf{I}, \mathbf{D}' = \mathbf{D}, \text{ and } \mathbf{B}' = \mathbf{B} . \quad (11)$$

781 On the other hand, the identifiability results for the causal ordering \mathbf{P} (or causal orderings \mathbf{P}^i) use
782 the following:

783 **Lemma 4** *Let \mathbf{P} and \mathbf{P}' be permutation matrices and \mathbf{T} and \mathbf{T}' be strictly lower triangular matrices,
784 such that $\mathbf{P}^\top \mathbf{T} \mathbf{P} = \mathbf{P}'^\top \mathbf{T}' \mathbf{P}'$. Assume that \mathbf{T} contains only non-zero elements in its strictly
785 lower triangular part. Then, $\mathbf{P} = \mathbf{P}'$ and $\mathbf{T} = \mathbf{T}'$.*

788 A.2 IDENTIFIABILITY OF LINGAM

789 As a special case, we restate here the identifiability of the single-view LiNGAM model (in terms of
790 the matrix \mathbf{B}).

791 **Theorem 5** (Identifiability of LiNGAM) *In the statistical model defined by Eq. 1, the parameter \mathbf{B}
792 is identifiable, provided that the entries in \mathbf{s} are mutually independent, that at most one of them is
793 Gaussian, and that \mathbf{B} is a DAG.*

794 This proof is based on the one from Shimizu et al. (2006), which we attempt to make a bit more rig-
795 orous. Identifiability was also shown in Shimizu (2022, Section 2.3) in the case with 2 components.

796 Let us transform the SEM

$$797 \mathbf{x} = \mathbf{B}\mathbf{x} + \mathbf{s} \quad (12)$$

800 into an ICA model

$$801 \mathbf{x} = \mathbf{A}\mathbf{s} \quad (13)$$

802 where the mixing matrix \mathbf{A} is constrained as $\mathbf{A}^{-1} = \mathbf{I} - \mathbf{B}$, and where \mathbf{B} is a DAG. The assumptions
803 on \mathbf{s} are identical in SEM and ICA. Let us parameterize by $\mathbf{W} = \mathbf{A}^{-1} = \mathbf{I} - \mathbf{B}$, instead of \mathbf{B} .

804 Consider two matrices $\mathbf{W} = \mathbf{I} - \mathbf{B}$ and $\mathbf{W}' = \mathbf{I} - \mathbf{B}'$, with \mathbf{B} and \mathbf{B}' being DAG matrices,
805 that parameterize the same statistical model in Eq. 12. We have $\det(\mathbf{W}) = \det(\mathbf{W}') = 1$, so
806 \mathbf{W} and \mathbf{W}' are invertible, which makes them valid unmixing matrices for the same ICA model in

Eq. 13. So, from the identifiability theory of ICA Comon (1994), we know that there exist a sign-permutation matrix \mathbf{Q} and a scaling matrix \mathbf{D} (*i.e.* a diagonal matrix with positive entries on the diagonal) such that

$$\mathbf{W}' = \mathbf{D}\mathbf{Q}^\top \mathbf{W} \quad (14)$$

hence

$$\mathbf{W}'' = \mathbf{Q}^\top \mathbf{W} \quad (15)$$

where we defined $\mathbf{W}'' = \mathbf{D}^{-1}\mathbf{W}'$. We thus have that $\mathbf{W}'' = \mathbf{D}^{-1}(\mathbf{I} - \mathbf{B}')$ and $\mathbf{W} = \mathbf{I} - \mathbf{B}$ both belong to the set \mathcal{W} , so applying Lemma 3 to \mathbf{W} and \mathbf{W}'' imposes $\mathbf{Q} = \mathbf{I}$, $\mathbf{D} = \mathbf{I}$, and $\mathbf{B}' = \mathbf{B}$. This makes \mathbf{B} fully identifiable (“fully” identifiable is in contrast to conventional ICA theory where some indeterminacies always remain), which concludes the proof.

A.3 PROOFS OF TECHNICAL LEMMAS

A.3.1 PROOF OF LEMMA 3

Consider $\mathbf{W}, \mathbf{W}' \in \mathcal{W}$ and \mathbf{Q} a sign-permutation matrix. Suppose that

$$\mathbf{W}' = \mathbf{Q}^\top \mathbf{W} . \quad (16)$$

A permutation inequality Using the definition of \mathcal{W} in Eq. 10 and the decompositions of DAG matrices, we have

$$\mathbf{W} = \mathbf{D}^{-1}\mathbf{P}^\top(\mathbf{I} - \mathbf{T})\mathbf{P} , \quad \mathbf{W}' = \mathbf{D}'^{-1}\mathbf{P}'^\top(\mathbf{I} - \mathbf{T}')\mathbf{P}' \quad (17)$$

where \mathbf{D}, \mathbf{D}' are diagonal matrices with positive entries on the diagonal, \mathbf{P}, \mathbf{P}' are permutation matrices, and \mathbf{T}, \mathbf{T}' are strictly lower triangular matrices. Denote $\mathbf{L} = \mathbf{I} - \mathbf{T}$ and $\mathbf{L}' = \mathbf{I} - \mathbf{T}'$; these are lower triangular matrices that have unit diagonals. We plug the decompositions into Eq. 16, and get

$$\mathbf{D}'^{-1}\mathbf{P}'^\top \mathbf{L}'\mathbf{P}' = \mathbf{Q}^\top \mathbf{D}^{-1}\mathbf{P}^\top \mathbf{L}\mathbf{P} . \quad (18)$$

To exploit the structure of the lower triangular matrices \mathbf{L} and \mathbf{L}' and show how they constrain \mathbf{Q} , we now switch notations from permutation — or sign-permutation — matrices $(\mathbf{P}, \mathbf{P}', \mathbf{Q})$, to their corresponding permutation functions (ϕ, ϕ', ψ) . Eq. 18 thus yields

$$\frac{\mathbf{L}'_{\phi'(i), \phi'(j)}}{\mathbf{D}'_{ii}} = \pm \frac{\mathbf{L}_{\phi(\psi(i)), \phi(j)}}{\mathbf{D}_{\psi(i), \psi(i)}} , \quad \forall i, j \in \llbracket 1, p \rrbracket \quad (19)$$

where the \pm symbol comes from \mathbf{Q} . In particular, \mathbf{L}' has unit diagonal, so

$$\mathbf{L}_{\phi(\psi(i)), \phi(i)} = \pm \frac{\mathbf{D}_{\psi(i), \psi(i)}}{\mathbf{D}'_{ii}} \neq 0 , \quad \forall i \in \llbracket 1, p \rrbracket \quad (20)$$

and \mathbf{L} is lower triangular, so that its non-zero entries must satisfy

$$\phi(i) \leq \phi(\psi(i)) , \quad \forall i \in \llbracket 1, p \rrbracket . \quad (21)$$

More generally, we can replace i with $\psi(i)$, and so on, and obtain

$$\phi(i) \leq \phi(\psi(i)) \leq \phi(\psi^{(2)}(i)) \leq \dots \quad \forall i \in \llbracket 1, p \rrbracket \quad (22)$$

where the superscript denotes composition and where we can apply the permutation ψ an arbitrary number of times.

Q must be a sign matrix Suppose that ψ is not the identity. We can pick an index $k \in \llbracket 1, p \rrbracket$ where $k \neq \psi(k)$. Because ϕ and ψ are injective, we can apply them to the inequality any number of times $n \in \mathbb{N}$ and get

$$\phi(\psi^{(n)}(k)) \neq \phi(\psi^{(n+1)}(k)) \quad (23)$$

which together with Eq. 22 implies

$$\phi(k) < \phi(\psi(k)) < \phi(\psi^{(2)}(k)) < \dots \quad (24)$$

which can be applied any number of times. However, each inequality increases the index by at least one, while the index cannot go above p . Thus, applying the chain at least p times, we have a contradiction. So, the permutation ψ in \mathbf{Q} must be the identity, and \mathbf{Q} boils down to a sign matrix, *i.e.* a diagonal matrix with 1 and -1 on the diagonal.

864
865
866
867
868
869
870
871
872
873
874
875
876
877
878
879
880
881
882
883
884
885
886
887
888
889
890
891
892
893
894
895
896
897
898
899
900
901
902
903
904
905
906
907
908
909
910
911
912
913
914
915
916
917

Q must be the identity Since $Q^\top = Q$, Eq. 18 can be reformulated as

$$P'^\top L' P' = D' Q D^{-1} P^\top L P \quad (25)$$

where we now know that $D' Q D^{-1}$ is a diagonal matrix. The matrix $P'^\top L' P'$ has a diagonal of ones and so too does $P^\top L P$. It follows that $D' Q D^{-1} = I$. Since D and D' have positive diagonal entries, it follows that the entries of Q cannot equal -1 . So, $Q = I$, and thus $D' = D$. This concludes the proof of the Lemma.

A.3.2 PROOF OF LEMMA 4

From the equality $P^\top T P = P'^\top T' P'$, we deduce that

$$T = \tilde{P}^\top T' \tilde{P} \quad (26)$$

where $\tilde{P} = P' P^\top$ is the permutation matrix represented by function ϕ , which is defined such that: $\forall k \in \llbracket 1, p \rrbracket$, $\tilde{P}_{k, \phi(k)} = 1$ and $\forall l \neq \phi(k)$, $\tilde{P}_{k, l} = 0$. Using the notation ϕ instead of \tilde{P} , Eq. 26 can be rewritten as, $\forall k, l \in \llbracket 1, p \rrbracket$,

$$T_{k, l} = T'_{\phi(k), \phi(l)} \quad (27)$$

We proceed by a proof by contradiction: assume that $\tilde{P} \neq I$. As a consequence, there exists an index k such that $\phi(k) \neq k$. Let us fix such an index as k . We can assume without loss of generality that

$$\phi(k) > k \quad (28)$$

otherwise we just have to invert signs and switch rows and columns in the following. By assumption, the strictly lower triangular part of T only has non-zero elements, so we have

$$T_{\phi(k), k} \neq 0 \quad (29)$$

Yet, from Eq. 27, we know that $T_{\phi(k), k} = T'_{\phi(\phi(k)), \phi(k)}$ and all the non-zero elements of T' are in its strictly lower triangular part, which implies

$$\phi(\phi(k)) > \phi(k) \quad (30)$$

This logic can be applied repeatedly as in the preceding lemma's proof, and we see that

$$\phi(k) < \phi^{(2)}(k) < \phi^{(3)}(k) < \dots \quad (31)$$

Now, this leads to an infinite strictly increasing sequence, which is contradictory since the index cannot grow greater than p . So, $\tilde{P} = I$, which means that $P' P^\top P = P$, and thus, using the orthogonality of P ,

$$P' = P \quad (32)$$

It also follows that $T' = T$, which concludes the proof of Lemma 4.

918 B LIKELIHOOD-BASED CRITERION

919 B.1 BASIC SETTING

920 The fundamental question here is to choose the causal direction for two variables, having many
 921 views i . We denote the two variables by x and y to avoid too many indices. It could be that the
 922 causal direction is $x \rightarrow y$:

$$923 y^i = b_i x^i + e^i \quad \text{for all } i \quad (33)$$

924 or $y \rightarrow x$:

$$925 x^i = c_i y^i + d^i \quad \text{for all } i . \quad (34)$$

926 Recall that superscripts are for view in the case of the random variables; however, for the re-
 927 gression coefficients we use subscripts because we need to take squares of such quantities. For
 928 the direction $x \rightarrow y$, collect the regressor and residuals in the vectors $\mathbf{x} = (x^1, \dots, x^m)^\top$ and
 929 $\mathbf{e} = (e^1, \dots, e^m)^\top$, respectively; and likewise for \mathbf{y} and \mathbf{d} in the opposite direction. Second-order
 930 moment matrices are denoted by $\Sigma_x = \mathbb{E}[\mathbf{x}\mathbf{x}^\top]$, $\Sigma_y = \mathbb{E}[\mathbf{y}\mathbf{y}^\top]$, and likewise for \mathbf{d} and \mathbf{e} . Note that
 931 the independence between \mathbf{x} and \mathbf{e} and between \mathbf{y} and \mathbf{d} , and the fact that \mathbf{x} and \mathbf{y} are standardized,
 932 imply that

$$933 b_i = c_i = \text{cov}(x_i, y_i) \quad \text{for all } i . \quad (35)$$

934 B.2 DERIVATION OF THE EXPECTED LOG-LIKELIHOOD IN ONE DIRECTION

935 We start by formulating the likelihood of the model in the case where disturbances are assumed to
 936 be Gaussian.

937 Consider the log-likelihood of (\mathbf{x}, \mathbf{y}) for the direction $x \rightarrow y$. Under the model, the prior (marginal)
 938 distribution of \mathbf{x} is $\mathcal{N}(\mathbf{0}, \Sigma_x)$, and the prior distribution of $\mathbf{e} = \mathbf{y} - \mathbf{b} \odot \mathbf{x}$ is $\mathcal{N}(\mathbf{0}, \Sigma_e)$ — where \odot
 939 denotes the elementwise product. Thus, we have

$$940 \begin{aligned} \log p(\mathbf{x}, \mathbf{y}; \mathbf{b}, \Sigma_x, \Sigma_e, x \rightarrow y) &= \log p(\mathbf{y}|\mathbf{x}; \mathbf{b}, \Sigma_x, \Sigma_e, x \rightarrow y) + \log p(\mathbf{x}; \mathbf{b}, x \rightarrow y) \\ 941 &= -(\mathbf{y} - \mathbf{b} \odot \mathbf{x})^\top \Sigma_e^{-1} (\mathbf{y} - \mathbf{b} \odot \mathbf{x}) - \log |\Sigma_e| - \mathbf{x}^\top \Sigma_x^{-1} \mathbf{x} - \log |\Sigma_x| \\ 942 &= -\text{tr}(\Sigma_e^{-1} (\mathbf{y} - \mathbf{b} \odot \mathbf{x})(\mathbf{y} - \mathbf{b} \odot \mathbf{x})^\top) - \log |\Sigma_e| - \text{tr}(\Sigma_x^{-1} \mathbf{x}\mathbf{x}^\top) - \log |\Sigma_x| \end{aligned} \quad (36)$$

943 where tr is the trace operator, and where we neglect the part of the normalization constant that does
 944 not depend on any parameters.

945 The expected log-likelihood is thus

$$946 \mathbb{E}[\log p(\mathbf{x}, \mathbf{y}; \mathbf{b}, \Sigma_x, \Sigma_e, x \rightarrow y)] = -\text{tr}(\Sigma_e^{-1} \mathbb{E}[(\mathbf{y} - \mathbf{b} \odot \mathbf{x})(\mathbf{y} - \mathbf{b} \odot \mathbf{x})^\top]) - \log |\Sigma_e| \quad (37)$$

$$947 -\text{tr}(\Sigma_x^{-1} \mathbb{E}[\mathbf{x}\mathbf{x}^\top]) - \log |\Sigma_x| \quad (38)$$

$$948 = -\log |\Sigma_x| - \log |\Sigma_e| - 2m . \quad (39)$$

949 Denote by \mathcal{L} this expected log-likelihood. We have (up to constants):

$$950 \mathcal{L}(\Sigma_x, \Sigma_e; x \rightarrow y) = -\log |\Sigma_x| - \log |\Sigma_e| . \quad (40)$$

951 B.3 DERIVATION OF THE LIKELIHOOD-BASED CRITERION

952 We now derive a criterion that can be used to find the causal direction.

953 The expected log-likelihood of the model for the direction $y \rightarrow x$ can be obtained by switching the
 954 roles of x and y in Eq. 40. Thus, we have

$$955 \mathcal{L}(\Sigma_y, \Sigma_d; y \rightarrow x) = -\log |\Sigma_y| - \log |\Sigma_d| \quad (41)$$

956 where we recall that $\Sigma_y = \mathbb{E}[\mathbf{y}\mathbf{y}^\top]$ and $\Sigma_d = \mathbb{E}[\mathbf{d}\mathbf{d}^\top]$.

957 The correct direction can then be found by comparing the expected log-likelihoods of both direc-
 958 tions. In particular, we calculate the difference between the two log-likelihoods, which can be
 959 reformulated as a likelihood ratio (LR):

$$960 \text{LR} := \mathcal{L}(\Sigma_x, \Sigma_e; x \rightarrow y) - \mathcal{L}(\Sigma_y, \Sigma_d; y \rightarrow x) = \mathbb{E} \left[\log \frac{p(\mathbf{x}, \mathbf{y}; \mathbf{b}, \Sigma_x, \Sigma_e, x \rightarrow y)}{p(\mathbf{x}, \mathbf{y}; \mathbf{c}, \Sigma_y, \Sigma_d, y \rightarrow x)} \right] . \quad (42)$$

Using Eq. 40 and Eq. 41, the criterion LR becomes

$$\text{LR} = -\log |\Sigma_x| - \log |\Sigma_e| + \log |\Sigma_y| + \log |\Sigma_d| . \quad (43)$$

Intuitively, the criterion in Eq. 43 will be large if the x^i are highly correlated (more than the y^i) over the views, since then the first determinant will be small. This should make intuitive sense since it means the cause is highly structured. Likewise, if the residuals for $x \rightarrow y$ are highly structured, that direction is more likely. In other words, the direction that exhibits more structure wins.

Surprisingly, in this formulation, there is actually no particular model for the dependencies of the disturbances: the likelihood should simply prefer dependent disturbances. It is important to note that the criterion makes sense even if the distribution is non-Gaussian, as will be proven below. We thus obtain a method that works for data of any distribution, but using only second-order statistics.

B.4 NON-NEGATIVITY OF THE LIKELIHOOD-BASED CRITERION

In this section, we prove that the criterion in Eq. 43 is non-negative for the direction $x \rightarrow y$. Importantly, no assumption of Gaussianity needs to be made here.

Consider the direction $x \rightarrow y$, and let us write $B := \text{diag}(b_1, \dots, b_m)$. Using the matrix B rather than the vector b makes notations clearer in the proofs. In the following, we use interchangeably b and B . The covariance matrix of $y = Bx + e$ is

$$\Sigma_y = B\Sigma_x B + \Sigma_e . \quad (44)$$

Given that $b_i = c_i$ for all i , we have $d = x - By = x - B(Bx + e) = (I - B)^2 x - Be$. Thus, the covariance matrix of d is

$$\Sigma_d = (I - B)^2 \Sigma_x (I - B)^2 + B\Sigma_e B . \quad (45)$$

Using these expressions, the criterion in Eq. 43 becomes

$$\text{LR} = -\log |\Sigma_x| - \log |\Sigma_e| + \log |B\Sigma_x B + \Sigma_e| + \log |(I - B)^2 \Sigma_x (I - B)^2 + B\Sigma_e B| . \quad (46)$$

Collect the variances of the residuals e in the diagonal matrix

$$L := \text{diag} \left(\sqrt{\text{var}(e^1)}, \dots, \sqrt{\text{var}(e^m)} \right) \quad (47)$$

and define the correlation matrix of the residuals as $\widetilde{\Sigma}_e$, so that

$$\Sigma_e = L\widetilde{\Sigma}_e L . \quad (48)$$

Now, the objective becomes

$$\begin{aligned} \text{LR} = & -\log |\Sigma_x| - \log |\widetilde{\Sigma}_e| - \log |L^2| + \log |B\Sigma_x B + L\widetilde{\Sigma}_e L| \\ & + \log |(I - B)^2 \Sigma_x (I - B)^2 + BL\widetilde{\Sigma}_e LB| . \end{aligned} \quad (49)$$

Importantly, the fact that x and y are standardized means that Σ_x and Σ_y have unit diagonal, so Eq. 44 implies

$$L^2 + B^2 = I \quad (50)$$

and it follows that the diagonal entries of L and B are in $[-1, 1]$. Thus, we have

$$\text{LR} = -\log |\Sigma_x| - \log |\widetilde{\Sigma}_e| - \log |L^2| + \log |B\Sigma_x B + L\widetilde{\Sigma}_e L| + \log |L^2 \Sigma_x L^2 + LB\widetilde{\Sigma}_e BL| \quad (51)$$

$$= -\log |\Sigma_x| - \log |\widetilde{\Sigma}_e| + \log |B\Sigma_x B + L\widetilde{\Sigma}_e L| + \log |L\Sigma_x L + B\widetilde{\Sigma}_e B| \quad (52)$$

where L and B commuted in the first equality because they are diagonal.

The following lemma (proven in Appendix B.5) shows that this criterion is non-negative, and even positive under some assumptions.

Lemma 6 Let Σ_x and $\widetilde{\Sigma}_e$ be $m \times m$ real symmetric positive definite matrices with unit diagonal entries. Let $\mathbf{B} = \text{diag}(b_1, \dots, b_m)$ and $\mathbf{L} = \text{diag}(l_1, \dots, l_m)$ be diagonal matrices with entries in $[-1, 1]$, satisfying $\mathbf{B}^2 + \mathbf{L}^2 = \mathbf{I}$ (i.e. $b_i^2 + l_i^2 = 1$ for all i). Define the function

$$J(\mathbf{B}, \mathbf{L}) := -\log \det \Sigma_x - \log \det \widetilde{\Sigma}_e + \log \det (\mathbf{B}\Sigma_x\mathbf{B} + \mathbf{L}\widetilde{\Sigma}_e\mathbf{L}) + \log \det (\mathbf{L}\Sigma_x\mathbf{L} + \mathbf{B}\widetilde{\Sigma}_e\mathbf{B}). \quad (53)$$

Under the above assumptions, we have $J(\mathbf{B}, \mathbf{L}) \geq 0$. Moreover, $J(\mathbf{B}, \mathbf{L}) = 0$ if and only if

$$\mathbf{L}\widetilde{\Sigma}_e\mathbf{B} = \mathbf{B}\Sigma_x\mathbf{L}. \quad (54)$$

B.5 PROOF OF A USEFUL LEMMA

Let us prove Lemma 6.

Step 1: define \mathbf{A} and \mathbf{C} — Define

$$\mathbf{A} := \mathbf{B}\Sigma_x\mathbf{B} + \mathbf{L}\widetilde{\Sigma}_e\mathbf{L} \quad \text{and} \quad \mathbf{C} := \mathbf{L}\Sigma_x\mathbf{L} + \mathbf{B}\widetilde{\Sigma}_e\mathbf{B}. \quad (55)$$

We have

$$J(\mathbf{B}, \mathbf{L}) := -\log \det \Sigma_x - \log \det \widetilde{\Sigma}_e + \log \det \mathbf{A} + \log \det \mathbf{C}. \quad (56)$$

Step 2: define \mathbf{M} — Define the $2m \times 2m$ block matrix

$$\mathbf{M} := \begin{pmatrix} \mathbf{B} & \mathbf{L} \\ -\mathbf{L} & \mathbf{B} \end{pmatrix}. \quad (57)$$

Since \mathbf{B} and \mathbf{L} are diagonal, they commute, hence $\mathbf{B}\mathbf{L} = \mathbf{L}\mathbf{B}$. Using $\mathbf{B}^2 + \mathbf{L}^2 = \mathbf{I}$, we compute

$$\mathbf{M}\mathbf{M}^\top = \begin{pmatrix} \mathbf{B}\mathbf{B} + \mathbf{L}\mathbf{L} & -\mathbf{B}\mathbf{L} + \mathbf{L}\mathbf{B} \\ -\mathbf{L}\mathbf{B} + \mathbf{B}\mathbf{L} & \mathbf{L}\mathbf{L} + \mathbf{B}\mathbf{B} \end{pmatrix} = \begin{pmatrix} \mathbf{I} & \mathbf{0} \\ \mathbf{0} & \mathbf{I} \end{pmatrix} = \mathbf{I}_{2m}. \quad (58)$$

Thus \mathbf{M} is orthonormal, so $\det \mathbf{M} = \pm 1$.

Step 3: define \mathcal{B} — Consider the block-diagonal matrix $\text{diag}(\Sigma_x, \widetilde{\Sigma}_e)$ and conjugate by \mathbf{M} :

$$\mathcal{B} := \mathbf{M} \begin{pmatrix} \Sigma_x & \mathbf{0} \\ \mathbf{0} & \widetilde{\Sigma}_e \end{pmatrix} \mathbf{M}^\top = \begin{pmatrix} \mathbf{A} & \mathbf{S} \\ \mathbf{S}^\top & \mathbf{C} \end{pmatrix}, \quad \mathbf{S} := \mathbf{L}\widetilde{\Sigma}_e\mathbf{B} - \mathbf{B}\Sigma_x\mathbf{L}. \quad (59)$$

Because \mathbf{M} is orthonormal and $\Sigma_x, \widetilde{\Sigma}_e \succ \mathbf{0}$, the matrix \mathcal{B} is symmetric positive definite (SPD). In particular, \mathbf{A} and \mathbf{C} are also SPD (as they are principal blocks of a SPD matrix) and thus \mathbf{A}^{-1} exists.

Step 4: Schur complement of \mathbf{A} in \mathcal{B} — For a symmetric block matrix $\begin{pmatrix} \mathbf{A} & \mathbf{S} \\ \mathbf{S}^\top & \mathbf{C} \end{pmatrix}$ with $\mathbf{A} \succ \mathbf{0}$, the Schur complement of \mathbf{A} is $\mathbf{C} - \mathbf{S}^\top \mathbf{A}^{-1} \mathbf{S}$, and the Schur's formula yields

$$\det \begin{pmatrix} \mathbf{A} & \mathbf{S} \\ \mathbf{S}^\top & \mathbf{C} \end{pmatrix} = \det(\mathbf{A}) \det(\mathbf{C} - \mathbf{S}^\top \mathbf{A}^{-1} \mathbf{S}). \quad (60)$$

Applying this to \mathcal{B} and using multiplicativity of determinant and the fact that $\det \mathbf{M} = \pm 1$ gives

$$\det(\Sigma_x) \det(\widetilde{\Sigma}_e) = \det(\mathcal{B}) = \det(\mathbf{A}) \det(\mathbf{C} - \mathbf{S}^\top \mathbf{A}^{-1} \mathbf{S}). \quad (61)$$

Step 5: derive a matrix inequality — Because $\mathcal{B} \succ \mathbf{0}$ and $\mathbf{A} \succ \mathbf{0}$, it follows from the Schur complement characterization of positive definiteness that $\mathbf{C} - \mathbf{S}^\top \mathbf{A}^{-1} \mathbf{S} \succ \mathbf{0}$. In particular, we have $\det(\mathbf{C} - \mathbf{S}^\top \mathbf{A}^{-1} \mathbf{S}) > 0$. Moreover, since $\mathbf{A} \succ \mathbf{0}$, we have $\mathbf{S}^\top \mathbf{A}^{-1} \mathbf{S} \succeq \mathbf{0}$, and thus $\mathbf{C} - \mathbf{S}^\top \mathbf{A}^{-1} \mathbf{S} \preceq \mathbf{C}$.

1080 **Step 6: derive a determinant inequality** — If $\mathbf{0} \preceq \mathbf{X} \preceq \mathbf{Y}$ and $\mathbf{Y} \succ \mathbf{0}$, then conjugating by
 1081 $\mathbf{Y}^{-1/2}$ shows $\mathbf{0} \preceq \mathbf{Y}^{-1/2} \mathbf{X} \mathbf{Y}^{-1/2} \preceq \mathbf{I}$. Thus, all eigenvalues of $\mathbf{Y}^{-1/2} \mathbf{X} \mathbf{Y}^{-1/2}$ lie in $[0, 1]$,
 1082 so their product satisfies $\det(\mathbf{Y}^{-1/2} \mathbf{X} \mathbf{Y}^{-1/2}) \leq 1$. Hence $\det(\mathbf{X}) \leq \det(\mathbf{Y})$. Applying this to
 1083 $\mathbf{X} := \mathbf{C} - \mathbf{S}^\top \mathbf{A}^{-1} \mathbf{S}$ and $\mathbf{Y} := \mathbf{C}$ yields

$$1084 \det(\mathbf{C} - \mathbf{S}^\top \mathbf{A}^{-1} \mathbf{S}) \leq \det(\mathbf{C}) . \quad (62)$$

1085
 1086 **Step 7: $J(\mathbf{B}, \mathbf{L}) \geq 0$** — From Steps 4 and 6, we get

$$1087 \det(\boldsymbol{\Sigma}_x) \det(\widetilde{\boldsymbol{\Sigma}}_e) = \det(\mathbf{A}) \det(\mathbf{C} - \mathbf{S}^\top \mathbf{A}^{-1} \mathbf{S}) \leq \det(\mathbf{A}) \det(\mathbf{C}) . \quad (63)$$

1088
 1089 Taking natural logarithms and rearranging gives

$$1090 \log \det(\mathbf{A}) + \log \det(\mathbf{C}) \geq \log \det(\boldsymbol{\Sigma}_x) + \log \det(\widetilde{\boldsymbol{\Sigma}}_e) , \quad (64)$$

1091
 1092 which is precisely $J(\mathbf{B}, \mathbf{L}) \geq 0$.

1093
 1094 **Step 8: equality condition** — The equality $J(\mathbf{B}, \mathbf{L}) = 0$ holds iff

$$1095 \det(\mathbf{C} - \mathbf{S}^\top \mathbf{A}^{-1} \mathbf{S}) = \det(\mathbf{C}) . \quad (65)$$

1096
 1097 Write $\mathbf{K} := \mathbf{C}^{-1/2} (\mathbf{S}^\top \mathbf{A}^{-1} \mathbf{S}) \mathbf{C}^{-1/2} \succeq \mathbf{0}$. We have

$$1098 \det(\mathbf{C} - \mathbf{S}^\top \mathbf{A}^{-1} \mathbf{S}) = \det(\mathbf{C}) \det(\mathbf{I} - \mathbf{C}^{-1} \mathbf{S}^\top \mathbf{A}^{-1} \mathbf{S}) \quad (66)$$

$$1099 = \det(\mathbf{C}) \det(\mathbf{C}^{-\frac{1}{2}} \mathbf{C}^{\frac{1}{2}} - \mathbf{C}^{-\frac{1}{2}} \mathbf{C}^{-\frac{1}{2}} \mathbf{S}^\top \mathbf{A}^{-1} \mathbf{S} \mathbf{C}^{-\frac{1}{2}} \mathbf{C}^{\frac{1}{2}}) \quad (67)$$

$$1100 = \det(\mathbf{C}) \det(\mathbf{C}^{-\frac{1}{2}}) \det(\mathbf{I} - \mathbf{K}) \det(\mathbf{C}^{\frac{1}{2}}) \quad (68)$$

$$1101 = \det(\mathbf{C}) \det(\mathbf{I} - \mathbf{K}) . \quad (69)$$

1102 Thus, the equality condition is $\det(\mathbf{I} - \mathbf{K}) = 1$. From Step 5, we know that $\mathbf{0} \preceq \mathbf{C} - \mathbf{S}^\top \mathbf{A}^{-1} \mathbf{S} \preceq$
 1103 \mathbf{C} . Conjugating by $\mathbf{C}^{-\frac{1}{2}}$ gives $\mathbf{0} \preceq \mathbf{I} - \mathbf{K} \preceq \mathbf{I}$, so each eigenvalue λ_i of \mathbf{K} satisfies $0 \leq \lambda_i \leq 1$.
 1104 The eigenvalues of $\mathbf{I} - \mathbf{K}$ are $1 - \lambda_i \in [0, 1]$, hence

$$1105 \prod_i (1 - \lambda_i) = \det(\mathbf{I} - \mathbf{K}) = 1 . \quad (70)$$

1106 The equality thus holds iff $\lambda_i = 0$ for all i , hence $\mathbf{K} = \mathbf{0}$. Since $\mathbf{C}^{-\frac{1}{2}}, \mathbf{A}^{-1} \succ \mathbf{0}$, we get $\mathbf{S} = \mathbf{0}$.
 1107 Conversely, $\mathbf{S} = \mathbf{0}$ clearly forces equality. Therefore, the equality occurs exactly when

$$1108 \mathbf{S} = \mathbf{L} \widetilde{\boldsymbol{\Sigma}}_e \mathbf{B} - \mathbf{B} \boldsymbol{\Sigma}_x \mathbf{L} = \mathbf{0} , \quad (71)$$

1109 *i.e.*

$$1110 \forall i, j : \quad b_i l_j (\boldsymbol{\Sigma}_x)_{ij} = l_i b_j (\widetilde{\boldsymbol{\Sigma}}_e)_{ij} . \quad (72)$$

1111 This completes the proof.

1112 B.6 CONDITIONS FOR STRICT POSITIVITY OF THE LIKELIHOOD-BASED CRITERION

1113 From now on, we assume that the model is not degenerate in the sense that disturbances have a
 1114 positive variance, that is $l_i = \text{var}(e_i) > 0$ for all i .

1115 The criterion LR derived in Appendix B.4 is used to determine the causal direction from its sign,
 1116 with LR = 0 indicating that the two directions cannot be distinguished. Lemma 6 shows that
 1117 LR = 0 if and only if

$$1118 \mathbf{L} \widetilde{\boldsymbol{\Sigma}}_e \mathbf{B} = \mathbf{B} \boldsymbol{\Sigma}_x \mathbf{L} . \quad (73)$$

1119 Entrywise, this is equivalent to

$$1120 \forall i, j : \quad l_i b_j (\widetilde{\boldsymbol{\Sigma}}_e)_{ij} = b_i l_j (\boldsymbol{\Sigma}_x)_{ij} . \quad (74)$$

1121 Let us fix $i, j \in \llbracket 1, m \rrbracket$.

1122 **Case 1: $b_i = 0$ and $b_j = 0$** — The equality immediately holds.

1134 **Case 2:** $b_i = 0$ and $b_j \neq 0$ — The right-hand side in Eq. 74 is equal to 0. Since $l_i = \text{var}(e^i) > 0$
 1135 and $b_j \neq 0$, we must have $(\widetilde{\Sigma}_e)_{ij} = 0$.
 1136

1137 **Case 3:** $b_i \neq 0$ and $b_j = 0$ — The left-hand side in Eq. 74 is equal to 0. Since $l_j = \text{var}(e^j) > 0$
 1138 and $b_i \neq 0$, we must have $(\Sigma_x)_{ij} = 0$.
 1139

1140 **Case 4:** $b_i \neq 0$ and $b_j \neq 0$ — Multiplying Eq. 74 by $\frac{l_j}{b_i b_j^2}$, and using $l_j^2 = 1 - b_j^2$, we obtain
 1141

$$1142 \frac{l_i l_j}{b_i b_j} (\widetilde{\Sigma}_e)_{ij} = \left(\frac{1}{b_j^2} - 1 \right) (\Sigma_x)_{ij} . \quad (75)$$

1143 Switching the roles of i and j , and using the symmetry of $(\widetilde{\Sigma}_e)_{ij}$ and $(\Sigma_x)_{ij}$, yield
 1144

$$1145 \frac{l_i l_j}{b_i b_j} (\widetilde{\Sigma}_e)_{ij} = \left(\frac{1}{b_i^2} - 1 \right) (\Sigma_x)_{ij} . \quad (76)$$

1146 hence

$$1147 b_i^2 (\Sigma_x)_{ij} = b_j^2 (\Sigma_x)_{ij} . \quad (77)$$

1148 Similarly, exchanging the roles of $(b_i, b_j, (\Sigma_x)_{ij})$ and $(l_i, l_j, (\widetilde{\Sigma}_e)_{ij})$ yields
 1149

$$1150 l_i^2 (\widetilde{\Sigma}_e)_{ij} = l_j^2 (\widetilde{\Sigma}_e)_{ij} . \quad (78)$$

1151 Now suppose $(\Sigma_x)_{ij} \neq 0$ or $(\widetilde{\Sigma}_e)_{ij} \neq 0$. From Eq. 77 and Eq. 78 it follows that $b_i^2 = b_j^2$ or $l_i^2 = l_j^2$.
 1152 Since $b_i^2 + l_i^2 = 1$, both equalities hold simultaneously:
 1153

$$1154 |b_i| = |b_j| \quad \text{and} \quad l_i = l_j \quad (79)$$

1155 where the absolute value can be dropped for l_i because $l_i = \text{var}(e_i) > 0$. Plugging these equalities
 1156 into Eq. 75 yields
 1157

$$1158 l_j^2 (\widetilde{\Sigma}_e)_{ij} = \pm (1 - b_j^2) (\Sigma_x)_{ij} \quad (80)$$

1159 hence

$$1160 |(\widetilde{\Sigma}_e)_{ij}| = |(\Sigma_x)_{ij}| . \quad (81)$$

1161 Moreover, for Eq. 74 to hold we must also have the sign equality
 1162

$$1163 \text{sign}(b_i) \text{sign}(b_j) = \text{sign}((\Sigma_x)_{ij}) \text{sign}((\widetilde{\Sigma}_e)_{ij}) . \quad (82)$$

1164 Altogether, either both $(\Sigma_x)_{ij}$ and $(\widetilde{\Sigma}_e)_{ij}$ vanish, or the following four conditions hold:
 1165

$$1166 |(\widetilde{\Sigma}_e)_{ij}| = |(\Sigma_x)_{ij}| \neq 0 \quad (83)$$

$$1167 |b_i| = |b_j| \quad (84)$$

$$1168 l_i = l_j \quad (85)$$

$$1169 \text{sign}(b_i) \text{sign}(b_j) = \text{sign}((\Sigma_x)_{ij}) \text{sign}((\widetilde{\Sigma}_e)_{ij}) . \quad (86)$$

1170 Conversely, if $(\Sigma_x)_{ij} = (\widetilde{\Sigma}_e)_{ij} = 0$, or if conditions Eq. 83–Eq. 86 are satisfied, then Eq. 74 holds.
 1171

1172 **Conclusion** — By contraposition, Eq. 73 is violated whenever there exists (i, j) such that one of
 1173 the following cases holds:
 1174

- 1175 • $b_i = 0, b_j \neq 0$, and $(\widetilde{\Sigma}_e)_{ij} \neq 0$
- 1176 • $b_i \neq 0, b_j = 0$, and $(\Sigma_x)_{ij} \neq 0$
- 1177 • $b_i \neq 0, b_j \neq 0, (\Sigma_x)_{ij} \neq 0$ or $(\widetilde{\Sigma}_e)_{ij} \neq 0$, and at least one of the conditions Eq. 83–Eq. 86
 1178 is not met.

1179 In particular, a simple sufficient condition is

$$1180 \exists i, j : \quad (b_i \neq 0 \quad \text{or} \quad b_j \neq 0) \quad \text{and} \quad |(\widetilde{\Sigma}_e)_{ij}| \neq |(\Sigma_x)_{ij}| . \quad (87)$$

1188 C CROSS-COVARIANCE-BASED CRITERION

1189 Consider the setting described in Appendix B.1.

1192 C.1 DERIVATION OF THE CROSS-COVARIANCE-BASED CRITERION

1194 A simple approach to infer the causal direction is to exploit the assumption that root variables and
 1195 residuals are independent. Specifically, if the true direction is $x \rightarrow y$, then \mathbf{x} and \mathbf{e} are independent;
 1196 if the true direction is $y \rightarrow x$, then \mathbf{y} and \mathbf{d} are independent. This implies that the cross-moment
 1197 matrix $\mathbb{E}[\mathbf{e}\mathbf{x}^\top]$ should vanish when $x \rightarrow y$, while $\mathbb{E}[\mathbf{d}\mathbf{y}^\top]$ should vanish when $y \rightarrow x$. Comparing
 1198 the Frobenius norms of these matrices therefore provides a natural criterion, based solely on cross-
 1199 covariances:

$$1200 \text{FC} := \left\| \mathbb{E}[\mathbf{d}\mathbf{y}^\top] \right\|_F - \left\| \mathbb{E}[\mathbf{e}\mathbf{x}^\top] \right\|_F . \quad (88)$$

1201 Intuitively, if this criterion is positive we deduce that $x \rightarrow y$, and if negative we deduce that $y \rightarrow x$.

1203 C.2 CONDITIONS FOR STRICT POSITIVITY OF THE CROSS-COVARIANCE CRITERION

1205 Assume without loss of generality that the true causal direction is $x \rightarrow y$, and let us analyze the sign
 1206 of the criterion FC.

1207 Given that $x \rightarrow y$, the true model is

$$1208 \mathbf{y} = \mathbf{B}\mathbf{x} + \mathbf{e} \quad (89)$$

1209 where $\mathbf{B} = \text{diag}(\text{cov}(x^1, y^1), \dots, \text{cov}(x^m, y^m))$, and \mathbf{e} is independent from \mathbf{x} . So, we have

$$1211 \mathbb{E}[\mathbf{x}\mathbf{e}^\top] = \mathbf{0} . \quad (90)$$

1212 In the wrong direction, the residuals take the form

$$1214 \mathbf{d} = \mathbf{x} - \mathbf{C}\mathbf{y}, \quad \mathbf{C} = \mathbf{B} . \quad (91)$$

1215 The cross-covariance between observations \mathbf{y} and residuals \mathbf{d} is then

$$1217 \mathbb{E}[\mathbf{y}\mathbf{d}^\top] = \mathbb{E}[\mathbf{y}(\mathbf{x} - \mathbf{B}\mathbf{y})^\top] \quad (92)$$

$$1218 = \mathbb{E}[(\mathbf{B}\mathbf{x} + \mathbf{e})(\mathbf{x} - \mathbf{B}(\mathbf{B}\mathbf{x} + \mathbf{e}))^\top] \quad (93)$$

$$1219 = \mathbb{E}[\mathbf{B}\mathbf{x}\mathbf{x}^\top(\mathbf{I} - \mathbf{B}^2)] + \mathbb{E}[\mathbf{e}\mathbf{x}^\top(\mathbf{I} - \mathbf{B}^2)] - \mathbb{E}[\mathbf{B}\mathbf{x}\mathbf{e}^\top\mathbf{B}] - \mathbb{E}[\mathbf{e}\mathbf{e}^\top\mathbf{B}] \quad (94)$$

$$1220 = \mathbf{B}\Sigma_x(\mathbf{I} - \mathbf{B}^2) - \Sigma_e\mathbf{B} \quad (95)$$

1221 where $\Sigma_x = \mathbb{E}[\mathbf{x}\mathbf{x}^\top]$ and $\Sigma_e = \mathbb{E}[\mathbf{e}\mathbf{e}^\top]$.

1222 From Eq. 90 and the non-negativity of the Frobenius norm, we see that FC is always non-negative.
 1223 Moreover, using Eq. 95, we deduce that FC = 0 if and only if

$$1224 \mathbf{B}\Sigma_x(\mathbf{I} - \mathbf{B}^2) - \Sigma_e\mathbf{B} = \mathbf{0} . \quad (96)$$

1225 Note that the fact that $l_i > 0$, for all i , makes \mathbf{L} invertible. So, using the identity $\mathbf{I} - \mathbf{B}^2 = \mathbf{L}^2$, and
 1226 multiplying on the right by \mathbf{L}^{-1} , we obtain

$$1227 \mathbf{B}\Sigma_x\mathbf{L} = \Sigma_e\mathbf{B}\mathbf{L}^{-1} \quad (97)$$

1228 hence

$$1229 \mathbf{B}\Sigma_x\mathbf{L} = \mathbf{L}\tilde{\Sigma}_e\mathbf{B} \quad (98)$$

1230 since $\Sigma_e = \mathbf{L}\tilde{\Sigma}_e\mathbf{L}$, and \mathbf{B} and \mathbf{L} commute.

1231 This condition coincides exactly with Eq. 73. In particular, this shows that the likelihood-based
 1232 criterion and the cross-covariance-based criterion share the same consistency assumptions.

1242 D IDENTIFIABILITY OF LIMVAM

1243 D.1 MULTIVARIATE CONDITIONS FOR STRICT POSITIVITY OF A CRITERION

1244 The following assumption is a multivariate generalization of the assumption detailed in B.6 and C.2.

1245 **Assumption 6** (Diversity of the views) *Let $j \neq j'$ denote any two component indices such that $\mathbf{x}_j \rightarrow \mathbf{x}_{j'}$. Then, there exist two views i and i' such that the three following conditions hold:*

1246 1. $\text{corr}(\mathbf{x}_j^i, \mathbf{x}_{j'}^i) \neq 0$ or $\text{corr}(\mathbf{x}_j^{i'}, \mathbf{x}_{j'}^{i'}) \neq 0$ 2. $\text{corr}(\mathbf{x}_j^i, \mathbf{x}_{j'}^{i'}) \neq 0$ or $\text{corr}(\mathbf{x}_j^{i'}, \mathbf{x}_{j'}^i) \neq 0$

1247 3. *At least one of the four following inequalities is met:*

1248 $|\text{corr}(\mathbf{x}_j^i, \mathbf{x}_{j'}^{i'})| \neq |\text{corr}(\mathbf{x}_j^{i'}, \mathbf{x}_{j'}^i)|$, $|\text{corr}(\mathbf{x}_j^i, \mathbf{x}_{j'}^i)| \neq |\text{corr}(\mathbf{x}_j^{i'}, \mathbf{x}_{j'}^{i'})|$, $\text{var}(\mathbf{e}_{j'}^i) \neq \text{var}(\mathbf{e}_{j'}^{i'})$
1249 $\text{sign}(\text{corr}(\mathbf{x}_j^i, \mathbf{x}_{j'}^i)) \text{sign}(\text{corr}(\mathbf{x}_j^{i'}, \mathbf{x}_{j'}^{i'})) \neq \text{sign}(\text{corr}(\mathbf{x}_j^i, \mathbf{x}_{j'}^{i'})) \text{sign}(\text{corr}(\mathbf{x}_j^{i'}, \mathbf{x}_{j'}^i))$

1250 where corr denotes the correlation coefficient and sign denotes the sign function.

1251 These conditions can only be met for indices $i \neq i'$, so they can be interpreted as a need for correlation and diversity across views. Because they may be hard to interpret at first glance, we next visualize in Figure 4 what these conditions mean for the causal graph.

1252 In particular, Assumption 6 immediately implies its simpler version used in the main text, Assumption 1.

1253 D.2 AN EXAMPLE FOR INTERPRETING THE SOS-BASED IDENTIFIABILITY CONDITION IN ASSUMPTION 1

1254 Consider one view and two variables denoted for notational simplicity x and y . We have

1255
$$y^1 = b^1 x^1 + e^1 \tag{99}$$

1256 and assume for simplicity that x^1 and y^1 have been standardized.

1257 Now, suppose we observe two datasets from this one view, denote them by (x^1, y^1) and $(x^{1'}, y^{1'})$, which have identical distributions and are independent of each other. Crucially, all this data is from one view. However, we could artificially generate a new “view” by adding those two datasets together:

1258
$$x^2 = x^1 + x^{1'} \tag{100}$$

1259 and likewise for y^2 and e^2 . Clearly the new data follows the SEM with the same b :

1260
$$y^2 = b^1 x^2 + e^2 \tag{101}$$

1261 since we are simply adding each of the terms separately in the two datasets.

1262 But this “multi-view” data is degenerate. In fact, the correlation coefficients are

1263
$$\text{corr}(x^1, x^2) = \frac{\text{cov}(x^1, x^1) + \text{cov}(x^1, x^{1'})}{\text{std}(x^1)\text{std}(x^2)} = \frac{\text{var}(x^1)}{\sqrt{2}\text{std}(x^1)\text{std}(x^1)} = \frac{1}{\sqrt{2}}. \tag{102}$$

1264 An exactly identical calculation applies for $\text{corr}(e^1, e^2)$ which is also equal to $1/\sqrt{2}$.

1265 Thus, we see that this case violates the simple identifiability condition in Assumption 1. This is understandable since no new information is created when computing the variable in the second view, and the two views are thus degenerate.

1296
1297
1298
1299
1300
1301
1302
1303
1304
1305
1306
1307
1308
1309
1310
1311
1312
1313
1314
1315
1316
1317
1318
1319
1320
1321
1322
1323
1324
1325
1326
1327
1328
1329
1330
1331
1332
1333
1334
1335
1336
1337
1338
1339
1340
1341
1342
1343
1344
1345
1346
1347
1348
1349

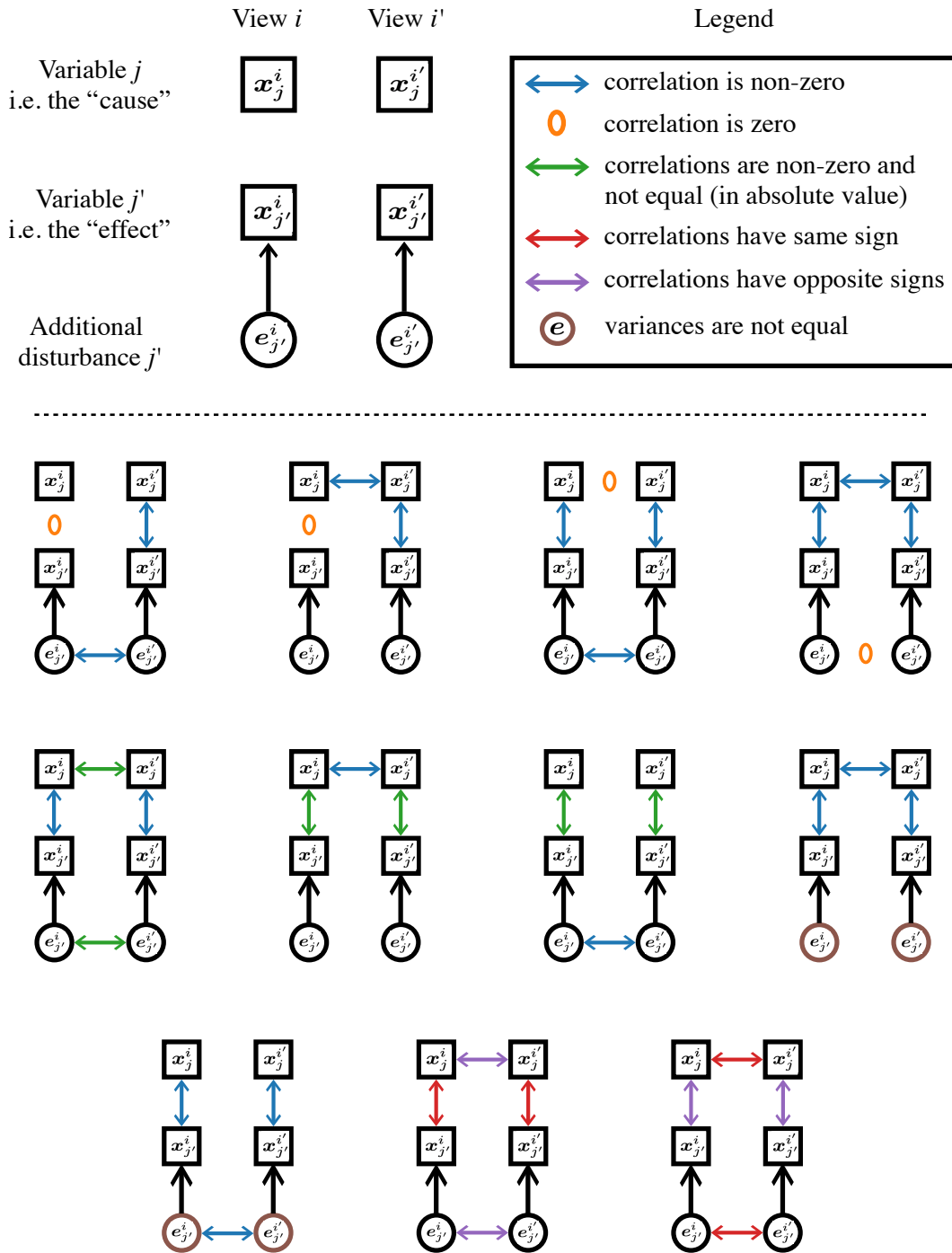


Figure 4: Assume the direction is $x_j \rightarrow x_{j'}$. Assumption 6 corresponds to being in one of the 11 situations showed in the figure. Note that no arrow means that no information is required.

D.3 PROOF OF THEOREM 1

We proceed in three steps. (i) We show that the LiMVAM model always admits at least one root variable and that our LR and FC criteria recover one consistently. (ii) We prove a *recursive residuals* lemma: removing a recovered root and regressing on it preserves the model form and the causal ordering, which implies that the full (partial) ordering is consistently recoverable. (iii) Conditional on the recovered ordering, each view-specific strictly lower-triangular system can be estimated consistently, hence the adjacency matrices are identifiable.

Preliminaries For clarity, we unpack the “shared ordering” assumption. This assumption is equivalent to the existence of a *main* DAG \mathcal{G} that is the union of view-specific DAGs $\{\mathcal{G}^i\}_{i=1}^m$: an edge appears in \mathcal{G} if it appears in at least one \mathcal{G}^i . Root variables are therefore common candidates across views. Furthermore, in terms of vocabulary, we distinguish (a) *directed paths* (a sequence of edges with consistent direction) from (b) *direct edges* (one edge between adjacent variables). An *indirect path* is a directed path with at least two edges.

D.3.1 RECOVERING A ROOT VARIABLE

Let observations follow LiMVAM in Eq. 3. Since all views share an ordering, there exists a (possibly non-unique) permutation \mathbf{P} such that

$$\mathbf{T}^i = \mathbf{P}^\top \mathbf{B}^i \mathbf{P} \quad \text{is strictly lower triangular for all } i \in \llbracket 1, m \rrbracket . \quad (103)$$

Reordering the observations and disturbances with $\mathbf{x}^i = \mathbf{P}\mathbf{x}^i$ and $\mathbf{e}^i = \mathbf{P}\mathbf{e}^i$, the model is

$$\mathbf{x}^i = \mathbf{T}^i \mathbf{x}^i + \mathbf{e}^i, \quad i \in \llbracket 1, m \rrbracket . \quad (104)$$

The first row of each \mathbf{T}^i is zero, so x_1^i is exogenous; hence a root variable always exists.

To *find* a root, consider distinct indices (j, k) and define M_{jk} to be the criterion from Eq. 5 or Eq. 6 (with $M_{kj} = -M_{jk}$). Stack these into $\mathbf{M} \in \mathbb{R}^{p \times p}$ with zero diagonal, and analyze signs under Assumption 6 (which concerns only direct relations):

1. **Direct edge:** $\mathbf{x}_j \rightarrow \mathbf{x}_k$ or $\mathbf{x}_k \rightarrow \mathbf{x}_j$. Under the bivariate conditions derived from Assumption 6, $M_{jk} > 0 > M_{kj}$ when $\mathbf{x}_j \rightarrow \mathbf{x}_k$, and $M_{jk} < 0 < M_{kj}$ when $\mathbf{x}_k \rightarrow \mathbf{x}_j$.
2. **Indirect path:** $\mathbf{x}_j \rightarrow \dots \rightarrow \mathbf{x}_k$ or $\mathbf{x}_k \rightarrow \dots \rightarrow \mathbf{x}_j$. Consider the reduced form of the model in Eq. 4, $\mathbf{x}^i = \mathbf{A}^i \mathbf{e}^i$ with $\mathbf{A}^i = (\mathbf{I} - \mathbf{B}^i)^{-1}$. The entry A_{kj}^i is the *total causal effect* of x_j^i on x_k^i , *i.e.* the sum over all directed paths from j to k of the products of edge coefficients. Hence for each view i ,

$$x_k^i = A_{kj}^i x_j^i + \epsilon^i \quad (105)$$

where ϵ^i collects all terms not caused by x_j^i and is independent of x_j^i . Thus, the pair (x_j^i, x_k^i) behaves as if there were a direct edge with coefficient A_{kj}^i , and the sign analysis of Item 1 applies but with non-strict inequalities: $M_{jk} \geq 0 \geq M_{kj}$ when $\mathbf{x}_j \rightarrow \dots \rightarrow \mathbf{x}_k$ (and conversely). If the bivariate conditions hold for (j, k) , the inequalities are strict; however, we do not require this here.

3. **No relation, no common ancestor:** then \mathbf{x}_j and \mathbf{x}_k depend on disjoint disturbance sets and are independent, hence $M_{jk} = M_{kj} = 0$.
4. **No relation but with a common ancestor.** If \mathbf{x}_j and \mathbf{x}_k are not connected by any directed path but share at least one ancestor, then their pairwise criteria M_{jk} and M_{kj} may take mixed signs. However, since each of \mathbf{x}_j and \mathbf{x}_k has at least one parent, there exist variables $\mathbf{x}_{j'}$ and $\mathbf{x}_{k'}$ such that $M_{jj'} < 0$ and $M_{kk'} < 0$. Thus, even if the signs of M_{jk} and M_{kj} are not determined, the j -th and k -th rows of \mathbf{M} necessarily contain negative entries. For instance, with three variables, $\mathbf{x}_1 \rightarrow \mathbf{x}_2$ and $\mathbf{x}_1 \rightarrow \mathbf{x}_3$ makes \mathbf{x}_2 and \mathbf{x}_3 siblings: there is no directed path between them, but both rows 2 and 3 of \mathbf{M} contain negative entries due to their direct parent \mathbf{x}_1 .

Consequently, \mathbf{x}_j is a root (no incoming edges) *if and only if* the j -th row of \mathbf{M} has only nonnegative entries. Hence a root exists and is consistently detectable. If multiple roots exist, we pick one at random.

1404 D.3.2 RECOVERING THE CAUSAL ORDERING

1405 We now show the recursive step.

1407 **Lemma 7** (Residuals preserve LiMVAM and the ordering) *Let j be a root variable. Regress every*
 1408 *other variable on x_j (within each view) and remove x_j . The residual vector still follows a LiMVAM*
 1409 *model with the same ordering over the remaining variables.*

1410 *Proof.* The proof is a direct adaptation of Shimizu et al. (2011, Lemma 2 and Corollary 1) to the
 1411 LiMVAM model: the original result is in the single-view setting with non-Gaussian disturbances.

1412 Choose a permutation P that places x_j first for simplicity (since x_j is a root variable, this permuta-
 1413 tion exists). In the permuted system we write

$$1414 \mathbf{x}'^i = \mathbf{T}^i \mathbf{x}'^i + \mathbf{e}'^i, \quad \mathbf{x}^i = P \mathbf{x}'^i, \quad \mathbf{e}^i = P \mathbf{e}'^i \quad (106)$$

1415 where each \mathbf{T}^i is strictly lower triangular and $\mathbf{x}'_1 = x_j$. Equivalently, the model can be expressed
 1416 in reduced form

$$1417 \mathbf{x}'^i = \mathbf{A}^i \mathbf{e}'^i, \quad \mathbf{A}^i := (\mathbf{I} - \mathbf{T}^i)^{-1} \quad (107)$$

1418 where the matrix \mathbf{A}^i is lower triangular with unit diagonal.

1419 The entry A_{k1}^i ($k \geq 2$) quantifies the dependence of x_k^i on e_1^i . Since $x'_1 = e_1^i$ is exogenous, we
 1420 have

$$1421 \mathbb{E}[x_k^i x_1^i] = A_{k1}^i \mathbb{E}[(x_1^i)^2] \quad (108)$$

1422 so the least-squares regression coefficient of x_k^i on x_1^i equals A_{k1}^i . Therefore, regressing each x_k^i
 1423 ($k \geq 2$) on x_1^i yields residuals $\mathbf{r}_{(1)}^i \in \mathbb{R}^{p-1}$ such that

$$1424 \mathbf{r}_{(1)}^i = \mathbf{x}'_{2:p}^i - \mathbf{A}_{2:p,1}^i x_1^i = \mathbf{A}_{2:p,:}^i \mathbf{e}'^i - \mathbf{A}_{2:p,1}^i e_1^i = \mathbf{A}_{2:p,2:p}^i \mathbf{e}'_{2:p}^i. \quad (109)$$

1425 Here $\mathbf{A}_{2:p,2:p}^i$ is again lower triangular with unit diagonal, and $\mathbf{e}'_{2:p}^i$ has mutually independent com-
 1426 ponents. Hence $\mathbf{r}_{(1)}^i$ follows a LiMVAM model on $p - 1$ variables. Moreover, since $\mathbf{A}_{2:p,2:p}^i$ is
 1427 precisely the submatrix of \mathbf{A}^i obtained by deleting the first row and column, the relative struc-
 1428 ture among the remaining variables is unchanged. In other words, the causal ordering of variables
 1429 $2, \dots, p$ is preserved. \square

1430 Applying Lemma 7 recursively — find a root via M (under Assumption 6), regress out its effect,
 1431 remove it, and repeat — recovers the full (partial) causal ordering consistently.

1432 D.3.3 RECOVERING THE ADJACENCY MATRICES

1433 Sections D.3.1 and D.3.2 showed that, under Assumption 6, the algorithms PairwiseLiMVAM and
 1434 DirectLiMVAM consistently recover the causal ordering. Equivalently, they recover a permutation
 1435 matrix P that makes the $\mathbf{T}^i = P^\top \mathbf{B}^i P$ strictly lower triangular. So, we can reorder the variables
 1436 as follows:

$$1437 \mathbf{x}'^i = \mathbf{T}^i \mathbf{x}'^i + \mathbf{e}'^i, \quad i \in \llbracket 1, m \rrbracket. \quad (110)$$

1438 Fix $j \in \llbracket 1, p \rrbracket$. We have

$$1439 x_j^i = \sum_{k=1}^{j-1} T_{jk}^i x_k^i + e_j^i, \quad i \in \llbracket 1, m \rrbracket. \quad (111)$$

1440 Because e_j^i is independent of $(x_1^i, \dots, x_{j-1}^i)$, the regressors are exogenous. This is a system of
 1441 linear regressions across views with potentially cross-view-correlated errors. Feasible GLS is con-
 1442 sistent in this setting: once a consistent estimate of the cross-view error covariance is obtained, the
 1443 GLS estimator converges to the true coefficients (Greene, 2003). Therefore, $\{T_{jk}^i\}_{k < j}$ are consis-
 1444 tently estimated for every (i, j) , hence each \mathbf{T}^i is consistently recovered. Finally, $\mathbf{B}^i = P \mathbf{T}^i P^\top$,
 1445 so the view-specific adjacency matrices are identifiable. This concludes the proof.

1456
 1457

1458 E SOS-BASED ALGORITHMS FOR LIMVAM

1459 E.1 CONSISTENT ESTIMATOR OF THE LIKELIHOOD-BASED CRITERION

1462 Assume we have observed n independent samples, concatenated as $\mathbf{X} = [\mathbf{x}_1, \dots, \mathbf{x}_n]$ and $\mathbf{Y} =$
 1463 $[\mathbf{y}_1, \dots, \mathbf{y}_n]$, with sample index j .

1464 In practice, the four covariance matrices in Eq. 43 can be estimated by consistent estimators from
 1465 the samples in \mathbf{X} and \mathbf{Y} . Since $b_i = c_i = \text{cov}(x_i, y_i)$ for all i , we define

$$1467 \quad \forall i : \quad \hat{b}_i := \hat{c}_i := \frac{1}{n} \sum_{j=1}^n x_{ij} y_{ij} \xrightarrow{p} \text{cov}(x_i, y_i) = b_i = c_i \quad (112)$$

1470 so that $\hat{\mathbf{b}} := (\hat{b}_1, \dots, \hat{b}_m)^\top \xrightarrow{p} \mathbf{b}$ and $\hat{\mathbf{c}} := (\hat{c}_1, \dots, \hat{c}_m)^\top \xrightarrow{p} \mathbf{c}$. Using these vectors, we define
 1471 the empirical covariances of the residuals

$$1472 \quad \widehat{\Sigma}_e := \frac{1}{n} \sum_{j=1}^n (\mathbf{y}_j - \hat{\mathbf{b}} \odot \mathbf{x}_j)(\mathbf{y}_j - \hat{\mathbf{b}} \odot \mathbf{x}_j)^\top \xrightarrow{p} \Sigma_e \quad (113)$$

$$1475 \quad \widehat{\Sigma}_d := \frac{1}{n} \sum_{j=1}^n (\mathbf{x}_j - \hat{\mathbf{b}} \odot \mathbf{y}_j)(\mathbf{x}_j - \hat{\mathbf{b}} \odot \mathbf{y}_j)^\top \xrightarrow{p} \Sigma_d \quad (114)$$

1478 and we also define the empirical covariances of the observations

$$1480 \quad \widehat{\Sigma}_x := \frac{1}{n} \sum_{j=1}^n \mathbf{x}_j \mathbf{x}_j^\top \xrightarrow{p} \Sigma_x \quad (115)$$

$$1483 \quad \widehat{\Sigma}_y := \frac{1}{n} \sum_{j=1}^n \mathbf{y}_j \mathbf{y}_j^\top \xrightarrow{p} \Sigma_y . \quad (116)$$

1486 We can then evaluate the criterion in these estimators.

$$1487 \quad \widehat{\text{LR}} := \mathcal{L}(\widehat{\Sigma}_x, \widehat{\Sigma}_e; x \rightarrow y) - \mathcal{L}(\widehat{\Sigma}_y, \widehat{\Sigma}_d; y \rightarrow x) = -\log |\widehat{\Sigma}_x| - \log |\widehat{\Sigma}_e| + \log |\widehat{\Sigma}_y| + \log |\widehat{\Sigma}_d| \quad (117)$$

1489 and it follows that this empirical criterion is a consistent estimator of the true criterion:

$$1490 \quad \mathcal{L}(\widehat{\Sigma}_x, \widehat{\Sigma}_e; x \rightarrow y) - \mathcal{L}(\widehat{\Sigma}_y, \widehat{\Sigma}_d; y \rightarrow x) \xrightarrow{p} \mathcal{L}(\Sigma_x, \Sigma_e; x \rightarrow y) - \mathcal{L}(\Sigma_y, \Sigma_d; y \rightarrow x) =: \text{LR} . \quad (118)$$

1494 E.2 CONSISTENT ESTIMATOR OF THE CROSS-COVARIANCE-BASED CRITERION

1495 Assume we have observed n independent samples, concatenated as $\mathbf{X} = [\mathbf{x}_1, \dots, \mathbf{x}_n]$ and $\mathbf{Y} =$
 1496 $[\mathbf{y}_1, \dots, \mathbf{y}_n]$, with sample index j .

1497 In practice, the matrices $\mathbb{E}[\mathbf{e}\mathbf{x}^\top]$ and $\mathbb{E}[\mathbf{d}\mathbf{y}^\top]$ are estimated from the data. Performing univariate
 1498 least-squares regression of \mathbf{y} on \mathbf{x} (resp. \mathbf{x} on \mathbf{y}) yields the residual matrices $\widehat{\mathbf{E}} = [\widehat{\mathbf{e}}_1, \dots, \widehat{\mathbf{e}}_n]$
 1499 (resp. $\widehat{\mathbf{D}} = [\widehat{\mathbf{d}}_1, \dots, \widehat{\mathbf{d}}_n]$). The corresponding cross-covariance estimators are

$$1501 \quad \frac{1}{n} \sum_{j=1}^n \widehat{\mathbf{e}}_j \mathbf{x}_j^\top \xrightarrow{p} \mathbb{E}[\mathbf{e}\mathbf{x}^\top] \quad \text{and} \quad \frac{1}{n} \sum_{j=1}^n \widehat{\mathbf{d}}_j \mathbf{y}_j^\top \xrightarrow{p} \mathbb{E}[\mathbf{d}\mathbf{y}^\top] . \quad (119)$$

1504 Consequently, the empirical criterion

$$1505 \quad \widehat{\text{FC}} := \left\| \frac{1}{n} \sum_{j=1}^n \widehat{\mathbf{d}}_j \mathbf{y}_j^\top \right\|_F - \left\| \frac{1}{n} \sum_{j=1}^n \widehat{\mathbf{e}}_j \mathbf{x}_j^\top \right\|_F \quad (120)$$

1509 is a consistent estimator of the population criterion:

$$1510 \quad \widehat{\text{FC}} \xrightarrow{p} \left\| \mathbb{E}[\mathbf{d}\mathbf{y}^\top] \right\|_F - \left\| \mathbb{E}[\mathbf{e}\mathbf{x}^\top] \right\|_F =: \text{FC} . \quad (121)$$

1512 E.3 ALGORITHMS FOR ESTIMATING THE TWO CRITERIA

1513

1514 In this section, the observations $\mathbf{X}, \mathbf{Y} \in \mathbb{R}^{m \times n}$ lie in two dimensions: the m views, and the n
 1515 independent samples. We use the index i for the views, and k for the samples.

1516

1517

1518 **Algorithm 1** Likelihood-based criterion

1519 **Input:** Observations $\mathbf{X}, \mathbf{Y} \in \mathbb{R}^{m \times n}$ corresponding to two variables, residuals $\mathbf{E}, \mathbf{D} \in \mathbb{R}^{m \times n}$
 1520 corresponding to the directions $x \rightarrow y$ and $y \rightarrow x$, respectively.

1521

1522 1. Compute the covariance matrices for the direction $x \rightarrow y$:

1523

$$1524 \widehat{\Sigma}_x = \frac{1}{n} \sum_{j=1}^n \mathbf{X}_j \mathbf{X}_j^\top \quad \text{and} \quad \widehat{\Sigma}_e = \frac{1}{n} \sum_{j=1}^n \mathbf{E}_j \mathbf{E}_j^\top \quad (122)$$

1525

1526 and for the direction $y \rightarrow x$:

1527

$$1528 \widehat{\Sigma}_y = \frac{1}{n} \sum_{j=1}^n \mathbf{Y}_j \mathbf{Y}_j^\top \quad \text{and} \quad \widehat{\Sigma}_d = \frac{1}{n} \sum_{j=1}^n \mathbf{D}_j \mathbf{D}_j^\top . \quad (123)$$

1529

1530 2. Compute the likelihood based-criterion:

1531

$$1532 \widehat{\text{LR}} = -\log |\widehat{\Sigma}_x| - \log |\widehat{\Sigma}_e| + \log |\widehat{\Sigma}_y| + \log |\widehat{\Sigma}_d| . \quad (124)$$

1533

1534 **Output:** Likelihood-based criterion $\widehat{\text{LR}}$.

1535

1536

1537

1538 **Algorithm 2** Cross-covariance-based criterion

1539 **Input:** Observations $\mathbf{X}, \mathbf{Y} \in \mathbb{R}^{m \times n}$ corresponding to two variables, residuals $\mathbf{E}, \mathbf{D} \in \mathbb{R}^{m \times n}$
 1540 corresponding to the directions $x \rightarrow y$ and $y \rightarrow x$, respectively.

1541

1542 1. Compute the second-moment matrices

1543

$$1544 \mathbf{M}_1 = \frac{1}{n} \sum_{j=1}^n \mathbf{E}_j \mathbf{X}_j^\top \quad \text{and} \quad \mathbf{M}_2 = \frac{1}{n} \sum_{j=1}^n \mathbf{D}_j \mathbf{Y}_j^\top . \quad (125)$$

1546

1547 2. Compute the cross-covariance-based criterion:

1548

$$1549 \widehat{\text{FC}} = \|\mathbf{M}_2\|_F - \|\mathbf{M}_1\|_F . \quad (126)$$

1550

1551 **Output:** Cross-covariance-based criterion $\widehat{\text{FC}}$.

1552

1553

1554

1555 E.4 HOW TO FIND THE ROOT VARIABLE

1556

1557 Assume we have a scalar criterion of the causal direction between two variables $\mathbf{x}_j =$
 1558 $(x_j^1, \dots, x_j^m)^\top$ and $\mathbf{x}_k = (x_k^1, \dots, x_k^m)^\top$, such that the criterion is positive if $\mathbf{x}_j \rightarrow \mathbf{x}_k$ and nega-
 1559 tive in the opposite direction. Let M_{jk} denote the criterion obtained for the pair (j, k) , and collect
 1560 all pairwise criteria in a matrix \mathbf{M} with a zero diagonal. We now have a matrix \mathbf{M} whose entries
 1561 determine the causal direction by their sign: $M_{ij} > 0$ indicates \mathbf{x}_i causes \mathbf{x}_j , and $M_{ij} < 0$ indicates
 1562 that \mathbf{x}_j causes \mathbf{x}_i . In this setting, \mathbf{x}_j is a root variable if and only if the j -th row of \mathbf{M} contains only
 1563 non-negative entries. We follow Hyvärinen & Smith (2013, Section 3.2.2) to derive a principled
 1564 criterion for finding the root variable given \mathbf{M} . We next recall their argument.

1565

Suppose that the entries in \mathbf{M} follow a normal distribution, so that $M_{ij} \sim \mathcal{N}(\mu_{ij}, \sigma^2)$ where σ^2
 models the estimation error due to finite samples (and is supposed to be constant for simplicity).

1566 Then, the log-likelihood of \mathbf{x}_i being the root variable is
 1567

$$1568 \log \prod_{j=1}^p P(\mu_{ij} > 0 | M_{ij}) = \sum_{j=1}^p \log P\left(\frac{\mu_{ij} - M_{ij}}{\sigma} > \frac{-M_{ij}}{\sigma} | M_{ij}\right) \quad (127)$$

$$1570 = \sum_{j=1}^p \log \Phi\left(\frac{M_{ij}}{\sigma}\right) \approx \frac{-1}{2\sigma^2} \sum_{j=1}^p \min(0, M_{ij})^2 \quad (128)$$

1574 where Φ is the cumulative distribution function of a standardized Gaussian, whose log we then
 1575 approximated. We therefore obtain the index of the root variable using

$$1576 \arg \min_i \sum_{j=1}^p \min(0, M_{ij})^2 . \quad (129)$$

1580 E.5 ONE-STEP FEASIBLE GENERALIZED LEAST SQUARES (FGLS)

1581 The FGLS procedure begins with an Ordinary Least Squares (OLS) regression in each view to
 1582 obtain residuals (e_j^1, \dots, e_j^m) , which are then used to estimate the cross-view covariance of the
 1583 disturbances. In a second step, the OLS coefficients are adjusted via Generalized Least Squares
 1584 using this estimated covariance. In the population limit, this estimator coincides with OLS but is
 1585 asymptotically more efficient whenever disturbances are correlated across views, as is the case here.
 1586

1587 The estimation proceeds as follows. Assume we have observed n independent samples. Here, we
 1588 consider the model

$$1589 \mathbf{x}^i = \mathbf{T}^i \mathbf{x}^i + \mathbf{e}^i, \quad i \in \llbracket 1, m \rrbracket \quad (130)$$

1590 where \mathbf{x}^i and \mathbf{e}^i are the reordered observations and disturbances, respectively, and \mathbf{T}^i are strictly
 1591 lower triangular matrices. By construction, each variable x_j^i only depends on its predecessors
 1592 $\mathbf{x}_{<j}^i := (x_1^i, \dots, x_{j-1}^i)$.

1593 Fix a variable index $j \in \llbracket 1, p \rrbracket$. In view i , the structural equation reads

$$1595 x_j^i = \sum_{k=1}^{j-1} T_{jk}^i x_k^i + e_j^i . \quad (131)$$

1598 Stacking all views, we obtain the block regression model

$$1600 \mathbf{x}'_j = \mathbf{X}_{<j} \mathbf{T}_{<j} + \mathbf{e}'_j \quad (132)$$

1601 where

- 1602 • $\mathbf{x}'_j = (x_j^1, \dots, x_j^m)^\top \in \mathbb{R}^{mn}$ stacks all samples across the m views,
- 1603 • $\mathbf{X}_{<j} = \text{diag}(\mathbf{x}_{<j}^1, \dots, \mathbf{x}_{<j}^m) \in \mathbb{R}^{mn \times m(j-1)}$ is block-diagonal and contains the predeces-
 1604 sors,
- 1605 • $\mathbf{T}_{<j} = (\mathbf{T}_{j,<j}^1, \dots, \mathbf{T}_{j,<j}^m)^\top \in \mathbb{R}^{m(j-1)}$ collects the coefficients,
- 1606 • $\mathbf{e}'_j = (e_j^1, \dots, e_j^m)^\top \in \mathbb{R}^{mn}$ are disturbances.

1610 The disturbance vector \mathbf{e}'_j has covariance

$$1612 \Omega_j := \mathbb{E}[\mathbf{e}'_j (\mathbf{e}'_j)^\top] = \Sigma_{e_j} \otimes \mathbf{I}_n \in \mathbb{R}^{mn \times mn} \quad (133)$$

1614 where $\Sigma_{e_j} \in \mathbb{R}^{m \times m}$ captures cross-view covariances for component j .

1615 The one-step FGLS procedure is:

1616 1. *OLS step:*

$$1617 \widehat{\mathbf{T}}_{<j}^{\text{OLS}} = (\mathbf{X}_{<j}^\top \mathbf{X}_{<j})^{-1} \mathbf{X}_{<j}^\top \mathbf{x}'_j \quad (134)$$

1618 yielding residuals $\hat{\mathbf{e}}'_j = \mathbf{x}'_j - \mathbf{X}_{<j} \widehat{\mathbf{T}}_{<j}^{\text{OLS}}$.

1620
1621
1622
1623
1624
1625
1626
1627
1628
1629
1630
1631
1632
1633
1634
1635
1636
1637
1638
1639
1640
1641
1642
1643
1644
1645
1646
1647
1648
1649
1650
1651
1652
1653
1654
1655
1656
1657
1658
1659
1660
1661
1662
1663
1664
1665
1666
1667
1668
1669
1670
1671
1672
1673

2. *Covariance estimation:*

$$\widehat{\Sigma}_{e_j} = \frac{1}{n} \sum_{k=1}^n \hat{e}'_{j,k} (\hat{e}'_{j,k})^\top \quad (135)$$

where k denotes the sample index.

3. *FGLS update:*

$$\widehat{\mathbf{T}}_{<j}^{\text{FGLS}} = (\mathbf{X}_{<j}^\top \widehat{\Sigma}_{e_j}^{-1} \mathbf{X}_{<j})^{-1} \mathbf{X}_{<j}^\top \widehat{\Sigma}_{e_j}^{-1} \mathbf{x}'_j . \quad (136)$$

This estimator reduces to OLS if Σ_{e_j} is diagonal (no cross-view correlation). More generally, it achieves asymptotic efficiency by exploiting cross-view correlations.

E.6 FULL ALGORITHM

Algorithm 3 Pairwise-comparison algorithms for multi-view causal discovery

Input: Observations $\mathbf{X} \in \mathbb{R}^{m \times p \times n}$.

1. *Preprocess the data \mathbf{X} .* Subtract the mean over the samples axis.
2. *Estimate the causal ordering \mathbf{P} .*
 - (a) Perform pairwise regressions between each pair of variables, \mathbf{x}_j on \mathbf{x}_i , such that $i \neq j$. Compute the residuals $\mathbf{e}_{i \rightarrow j}$.
 - (b) Compute a skew-symmetric matrix $\mathbf{M} \in \mathbb{R}^{p \times p}$ that determines the causal direction between pairs of variables.

The entries M_{ij} are computed with Eq. 5 or Eq. 6 for all $i < j$, using the regression results $(\mathbf{x}_i, \mathbf{x}_j, \mathbf{e}_{i \rightarrow j}, \mathbf{e}_{j \rightarrow i})$. Then set $M_{ji} = -M_{ij}$. M_{ij} positive means \mathbf{x}_i causes \mathbf{x}_j , negative means \mathbf{x}_j causes \mathbf{x}_i .

- (c) Determine the root variable k : it causes all others, so M_{kj} should be positive for all j .

$$k = \operatorname{argmin}_i \sum_j \min(0, M_{ij})^2 . \quad (137)$$

- (d) Remove the root variable k and replace observations with residuals obtained when regressing on k . Repeat.
- (e) Store the estimated ordering in a permutation matrix \mathbf{P} , and reorder the variables in \mathbf{X} according to this permutation. This yields a new model $\mathbf{x}'^i = \mathbf{T}^i \mathbf{x}'^i + \mathbf{e}'^i$, where \mathbf{x}'^i and \mathbf{e}'^i are reordered versions of \mathbf{x}^i and \mathbf{e}^i , respectively, and the \mathbf{T}^i are strictly lower triangular matrices.

3. *Estimate the adjacency matrices \mathbf{B}^i .* For each variable $j \in [2, p]$, estimate the j -th row of all matrices \mathbf{T}^i with one-step Feasible Generalized Least Squares Zellner (1962). Recover matrices $\mathbf{B}^i = \mathbf{P}^\top \mathbf{T}^i \mathbf{P}$.

Output: Adjacency matrices $(\mathbf{B}^1, \dots, \mathbf{B}^m) \in \mathbb{R}^{m \times p \times p}$.

E.7 COMPUTATIONAL COMPLEXITY

The computational complexity of Algorithm 3 can be broken down across the different steps.

In Step 1, the preprocessing is in $O(m \cdot p \cdot n)$.

In Step 2.a., we solve $O(p^2)$ LS regression problems, each of which has complexity $O(m \cdot n)$.

In Step 2.b., we compute $O(p^2)$ entries of a matrix. Each entry is computed either using the cross-covariance-based criterion in Algorithm 2 which is in $O(m^2 \cdot n)$, or using the likelihood-based criterion in Algorithm 1 which is in $O(m^2 \cdot n + m^3)$ due to computing log determinants. So the total complexity of this step is $O(m^2 \cdot p^2 \cdot n)$ or $O(m^2 \cdot p^2 \cdot n + m^3 \cdot p^2)$.

In Step 2.c., we make $O(p^2)$ operations.

1674 In Step 2.d., we simplify redefine a matrix.
1675
1676 These steps 2.a-d., are repeated $O(p)$ times, until all variables are removed, so this yields a com-
1677 plexity in either $O(m^2 \cdot p^3 \cdot n)$ or $O(m^2 \cdot p^3 \cdot n + m^3 \cdot p^3)$.
1678 In Step 2.e., we reorder a matrix, which costs $O(m \cdot p \cdot n)$ operations.
1679
1680 In Step 3, we run the one-step Feasible GLS procedure, which is in $O(m^3 \cdot p^3 \cdot n)$. It scales cubically
1681 in the m views and p dimensions as it involves matrix multiplications and inversions. It then does
1682 m matrix multiplications. Each of them involves permutation matrices which has a quadratic cost
1683 $O(p^2)$. So the cost of this step is dominated by $O(m^3 \cdot p^3 \cdot n)$.
1684 The total computational complexity of the algorithm is thus $O(m^3 \cdot p^3 \cdot n)$.
1685
1686
1687
1688
1689
1690
1691
1692
1693
1694
1695
1696
1697
1698
1699
1700
1701
1702
1703
1704
1705
1706
1707
1708
1709
1710
1711
1712
1713
1714
1715
1716
1717
1718
1719
1720
1721
1722
1723
1724
1725
1726
1727

F IDENTIFIABILITY OF LIMVAM WITH SHARED DISTURBANCES

In this section, we analyze the identifiability of the LiMVAM model with shared disturbances

$$\mathbf{x}^i = \mathbf{B}^i \mathbf{x}^i + \mathbf{D}^i \mathbf{s} + \mathbf{n}^i, \quad i \in \llbracket 1, m \rrbracket \quad (138)$$

where the \mathbf{D}^i are diagonal matrices with positive entries on the diagonal, \mathbf{s} has mutually independent entries and second-order moment $\mathbb{E}[\mathbf{s}\mathbf{s}^\top] = \mathbf{I}_p$, the view-specific noises are Gaussian $\mathbf{n}^i \sim \mathcal{N}(\mathbf{0}, \Sigma^i)$ with diagonal Σ^i , and the vectors \mathbf{s} and $\mathbf{n}^i, i = 1, \dots, m$, are mutually independent.

F.1 PROOF OF THEOREM 2 (FIRST CLAIM)

Consider two sets $\Theta = (\mathbf{D}^1, \dots, \mathbf{D}^m, \Sigma^1, \dots, \Sigma^m, \mathbf{B}^1, \dots, \mathbf{B}^m)$ and $\Theta' = (\mathbf{D}'^1, \dots, \mathbf{D}'^m, \Sigma'^1, \dots, \Sigma'^m, \mathbf{B}'^1, \dots, \mathbf{B}'^m)$ that parameterize the same statistical model in Eq. 138, with \mathbf{D}^i and \mathbf{D}'^i being diagonal matrices with positive entries on the diagonal, Σ^i and Σ'^i being diagonal matrices with non-zero entries on the diagonal, and \mathbf{B}^i and \mathbf{B}'^i being DAG matrices. The model in Eq. 138 can be reformulated as

$$\mathbf{x}^i = (\mathbf{I} - \mathbf{B}^i)^{-1} \mathbf{D}^i (\mathbf{s} + (\mathbf{D}^i)^{-1} \mathbf{n}^i) \quad (139)$$

which corresponds to the Shared ICA model

$$\mathbf{x}^i = \mathbf{A}^i (\mathbf{s} + \tilde{\mathbf{n}}^i) \quad (140)$$

for $\mathbf{A}^i = (\mathbf{I} - \mathbf{B}^i)^{-1} \mathbf{D}^i$ and $\tilde{\mathbf{n}}^i = (\mathbf{D}^i)^{-1} \mathbf{n}^i$. We can observe that the unmixing matrices $\mathbf{W}^i = (\mathbf{A}^i)^{-1} = (\mathbf{D}^i)^{-1} (\mathbf{I} - \mathbf{B}^i)$ and $\mathbf{W}'^i = (\mathbf{A}'^i)^{-1} = (\mathbf{D}'^i)^{-1} (\mathbf{I} - \mathbf{B}'^i)$ belong to the domain \mathcal{W} , which is included in the space of invertible matrices. Thus, the two sets of \mathbf{W}^i and \mathbf{W}'^i matrices are valid sets of unmixing matrices for the same multi-view ICA model in Eq. 140. Moreover, Assumption 4 allows the rescaled noises $\tilde{\mathbf{n}}^i$ to meet the noise diversity condition of Shared ICA. So, from the identifiability theory of multi-view ICA (Richard et al., 2021, Theorem 1), we know that there exist a sign-permutation matrix \mathbf{Q} such that for any view $i \in \llbracket 1, m \rrbracket$, we have

$$\begin{aligned} \mathbf{W}'^i &= \mathbf{Q}^\top \mathbf{W}^i \\ \Sigma'^i &= \mathbf{Q}^\top \Sigma^i \mathbf{Q} . \end{aligned} \quad (141)$$

Note that, contrary to the single-view context, the fact that we obtain \mathbf{W} up to *sign* and permutation rather than *scale* and permutation is because $\mathbb{E}[\mathbf{s}\mathbf{s}^\top] = \mathbf{I}$. Then, we apply Lemma 3, which shows that being in the domain \mathcal{W} imposes $\mathbf{Q} = \mathbf{I}$, $\mathbf{D}'^i = \mathbf{D}^i$, and $\mathbf{B}'^i = \mathbf{B}^i$.

F.2 PROOF OF THEOREM 2 (SECOND CLAIM)

In the context of shared causal ordering \mathbf{P} , we prove that, under Assumptions 4 and 5, the decomposition of matrices \mathbf{B}^i into matrices \mathbf{T}^i and \mathbf{P} is unique.

Consider the two sets $\Theta = (\Sigma^1, \dots, \Sigma^m, \mathbf{P}, \mathbf{T}^1, \dots, \mathbf{T}^m)$ and $\Theta' = (\bar{\Sigma}^1, \dots, \bar{\Sigma}^m, \bar{\mathbf{P}}, \bar{\mathbf{T}}^1, \dots, \bar{\mathbf{T}}^m)$ that parameterize the same statistical model in Eq. 138, where \mathbf{P} is some permutation matrix, \mathbf{T}^i are strictly lower triangular matrices, and $\bar{\mathbf{P}}$ and $\bar{\mathbf{T}}^i$ are the particular matrices given by Assumption 5. Note that no assumption on the sparsity of the \mathbf{T}^i is made. From Theorem 2, we know that $\Sigma^i = \bar{\Sigma}^i$.

Assumption 5 amounts to saying that the “reunion” of the $\bar{\mathbf{T}}^i$ represents a fully connected graph. In other words, if we define the reunion as $\bar{\mathbf{T}}^U = \sum_{i=1}^m \text{abs}(\bar{\mathbf{T}}^i)$, where abs denotes the element-wise absolute value function, then we are assuming that the strictly lower triangular part of $\bar{\mathbf{T}}^U$ only has non-zero elements. In a similar way to the definition of $\bar{\mathbf{T}}^U$, let us define

$$\bar{\mathbf{W}}^U = \sum_{i=1}^m \text{abs}(\bar{\mathbf{W}}^i) \quad (142)$$

where $\bar{\mathbf{W}}^i = \mathbf{I} - \bar{\mathbf{P}}^\top \bar{\mathbf{T}}^i \bar{\mathbf{P}}$. The non-zero elements of $\bar{\mathbf{P}}^\top \bar{\mathbf{T}}^i \bar{\mathbf{P}}$ are outside of the diagonal, so matrices \mathbf{I} and $\bar{\mathbf{P}}^\top \bar{\mathbf{T}}^i \bar{\mathbf{P}}$ contain non-zero elements at different locations. Thus, we have

$$\text{abs}(\mathbf{I} - \bar{\mathbf{P}}^\top \bar{\mathbf{T}}^i \bar{\mathbf{P}}) = \mathbf{I} + \text{abs}(\bar{\mathbf{P}}^\top \bar{\mathbf{T}}^i \bar{\mathbf{P}}) . \quad (143)$$

Furthermore, applying $\bar{\mathbf{P}}$ to the rows and columns of $\bar{\mathbf{T}}^i$ only shuffles its entries, without modifying their values. So we have

$$\text{abs}(\bar{\mathbf{P}}^\top \bar{\mathbf{T}}^i \bar{\mathbf{P}}) = \bar{\mathbf{P}}^\top \text{abs}(\bar{\mathbf{T}}^i) \bar{\mathbf{P}} . \quad (144)$$

Consequently,

$$\bar{\mathbf{W}}^U = \sum_{i=1}^m \mathbf{I} + \bar{\mathbf{P}}^\top \text{abs}(\bar{\mathbf{T}}^i) \bar{\mathbf{P}} = \sum_{i=1}^m \bar{\mathbf{P}}^\top (\mathbf{I} + \text{abs}(\bar{\mathbf{T}}^i)) \bar{\mathbf{P}} = \bar{\mathbf{P}}^\top (m\mathbf{I} + \bar{\mathbf{T}}^U) \bar{\mathbf{P}} . \quad (145)$$

So, dividing both sides by m gives

$$\frac{1}{m} \bar{\mathbf{W}}^U = \bar{\mathbf{P}}^\top \left(\mathbf{I} - \left(-\frac{1}{m} \bar{\mathbf{T}}^U \right) \right) \bar{\mathbf{P}} \quad (146)$$

where $-\frac{1}{m} \bar{\mathbf{T}}^U$ is strictly lower triangular, and its strictly lower triangular part only has non-zero elements.

Next, we apply the same reasoning to the alternative set of parameters, given by $\mathbf{W}^i = \mathbf{I} - \mathbf{P}^\top \mathbf{T}^i \mathbf{P}$, and we consider $\mathbf{W}^U = \sum_{i=1}^m \text{abs}(\mathbf{W}^i)$. The proof of Theorem 2 already implied that $\bar{\mathbf{W}}^i = \mathbf{W}^i$ for all i . Thus, we have $\bar{\mathbf{W}}^U = \mathbf{W}^U$ and

$$\bar{\mathbf{P}}^\top \left(\mathbf{I} - \left(-\frac{1}{m} \bar{\mathbf{T}}^U \right) \right) \bar{\mathbf{P}} = \mathbf{P}^\top \left(\mathbf{I} - \left(-\frac{1}{m} \mathbf{T}^U \right) \right) \mathbf{P} \quad (147)$$

where \mathbf{T}^U is defined in a similar way as $\bar{\mathbf{T}}^U$, except that its strictly lower triangular part can be sparse. Using Lemma 4 on Eq. 147, we obtain that $\mathbf{P} = \bar{\mathbf{P}}$, and thus $\mathbf{T}^i = \bar{\mathbf{T}}^i$ for all i . In conclusion, all the sets of DAG decompositions that parameterize the same model are equal, as soon as for one of these decompositions, the reunion of the \mathbf{T}^i is dense. We conclude that matrices \mathbf{P} and \mathbf{T}^i are unique, and thus identifiable in our terminology. This proof also implies that there can be only one matrix $\bar{\mathbf{P}}$ that fulfills Assumption 5.

F.3 RESULTS FOR VIEW-SPECIFIC CAUSAL ORDERINGS

Next, we consider a case which is outside of the theory of the main paper, although a simple extension: we allow the causal orderings to be different in different views. It turns out that in the view-specific \mathbf{P}^i case, identifiability is obtained by assuming that the directed acyclic graph \mathbf{B}^i is dense enough in each view, as formalized in the following assumption. However, since the \mathbf{B}^i can be permuted to strictly lower triangular matrices, they cannot be denser than having $\frac{p(p-1)}{2}$ non-zero entries.

Assumption 7 (Dense connectivity in each view) *For each view i , the matrix \mathbf{B}^i has exactly $\frac{p(p-1)}{2}$ non-zero entries.*

Using Assumption 7, the following theorem states that, in addition to identifying \mathbf{B}^i , \mathbf{D}^i , and Σ^i , one can also identify \mathbf{T}^i and \mathbf{P}^i .

Theorem 8 (Identifiability of multiple causal orderings) *Consider the LiMVAM model with multiple causal orderings. Consider the quantities $(\mathbf{D}^1, \dots, \mathbf{D}^m, \Sigma^1, \dots, \Sigma^m, \mathbf{P}^1, \dots, \mathbf{P}^m, \mathbf{T}^1, \dots, \mathbf{T}^m)$ as the set of parameters to be estimated. Under Assumptions 4 and 7, all these parameters are identifiable.*

In the context of view-specific causal orderings \mathbf{P}^i , we prove that, under Assumptions 4 and 7, the decomposition of matrices \mathbf{B}^i into matrices \mathbf{T}^i and \mathbf{P}^i is unique.

Consider two sets of parameters $\Theta = (\Sigma^1, \dots, \Sigma^m, \mathbf{P}^1, \dots, \mathbf{P}^m, \mathbf{T}^1, \dots, \mathbf{T}^m)$ and $\Theta' = (\Sigma'^1, \dots, \Sigma'^m, \mathbf{P}'^1, \dots, \mathbf{P}'^m, \mathbf{T}'^1, \dots, \mathbf{T}'^m)$ that parameterize the same statistical model in Eq. 138, where $\mathbf{P}^i, \mathbf{P}'^i$ are permutation matrices, and $\mathbf{T}^i, \mathbf{T}'^i$ are strictly lower triangular matrices. Note that here we parameterize by \mathbf{P}^i and \mathbf{T}^i rather than \mathbf{B}^i or \mathbf{W}^i . From Theorem 2, we know that $\Sigma^i = \Sigma'^i$ and that the resulting causal matrices must be equal:

$$(\mathbf{P}^i)^\top \mathbf{T}^i \mathbf{P}^i = (\mathbf{P}'^i)^\top \mathbf{T}'^i \mathbf{P}'^i . \quad (148)$$

Assumption 7 states that, for each view i , the matrix $\mathbf{B}^i = (\mathbf{P}^i)^\top \mathbf{T}^i \mathbf{P}^i = (\mathbf{P}'^i)^\top \mathbf{T}'^i \mathbf{P}'^i$ contains exactly $\frac{p(p-1)}{2}$ non-zero elements, so it is also the case for \mathbf{T}^i and \mathbf{T}'^i which thus represent fully connected graphs. So, from Lemma 4, we deduce that, for each view i , we have $\mathbf{P}^i = \mathbf{P}'^i$ and $\mathbf{T}^i = \mathbf{T}'^i$, which concludes the proof.

1836 G ICA-BASED ALGORITHM FOR LIMVAM WITH SHARED DISTURBANCES

1837 G.1 ICA-BASED ALGORITHM

1840 **Algorithm 4** ICA-LiMVAM

1842 1. *Estimate the adjacency matrices B^i .*

1843 (a) Estimate the unmixing matrices W^i and the noise variance matrices Σ^i , by running
1844 the Shared ICA estimation algorithm on the data.

1845 The algorithm returns an estimate of the true unmixing matrix $W^i = M(I - B^i)$ but
1846 up to sign-permutation matrix M that is the same for all views (Richard et al., 2021).

1847 (b) Determine the sign-permutation indeterminacy M , using the structure of the under-
1848 lying $(A^i)^{-1}$ that has a diagonal of ones. Thus, we can adapt the simple two-step
1849 heuristic by Shimizu et al. (2006).

1850 First, find a permutation matrix M such that MW has a non-zero diagonal, by solv-
1851 ing with the Hungarian algorithm

$$1852 \min_M \sum_{j=1}^p \frac{1}{|(MW)_{jj}|}, \quad W = \sum_{i=1}^m \text{abs}(W^i), \quad (149)$$

1853 and then rescale the rows of M to ensure that MW has a diagonal of ones

$$1854 M_{ij} \leftarrow \text{sign}((MW)_{ii})M_{ij}, \quad (150)$$

1855 where the sign function outputs 1 or -1 .

1856 (c) Determine the scale matrices $D^i = \text{diag}\left(\frac{1}{(MW^i)_{11}}, \dots, \frac{1}{(MW^i)_{pp}}\right)$.

1857 (d) Determine the causal matrices $B^i = I - D^i MW^i$ and update the noise variance
1858 matrices with $\Sigma^i \leftarrow (D^i)^2 \Sigma^i$.

1859 2. *Determine the causal ordering P .*

1860 The DAG decomposition states that $B^i := P^\top T^i P$ where T^i is lower triangular, so we
1861 penalize for that

$$1862 \min_P \sum_{l \geq k} (PBP^\top)_{kl}^2, \quad B = \sum_{i=1}^m \text{abs}(B^i). \quad (151)$$

1863 We approximately minimize this objective using the heuristic algorithm presented
1864 in Shimizu et al. (2006, Algorithm C).

1874 Note that the algorithm described in Chen et al. (2024) finds the same adjacency matrices as we do.
1875 This is because of the sign-permutation matrix M from ICA: to determine that matrix, we ensure
1876 MW has a diagonal of ones by dividing by the scalings D^i . For Chen et al. (2024), these scalings
1877 are not part of the model: they are simply a part of the algorithm which determines M . For us, these
1878 scalings are part of our model.

1880 G.2 COMPUTATIONAL COMPLEXITY

1881 We next detail the worst-case computational complexity of the ICA-LiMVAM algorithm which is
1882 in $O(tnmp^3 + mp^5)$, for t iterations of the SharedICA-ML algorithm, n samples, m views and p
1883 components. Note that the term in p^5 comes from Algorithm C of the original LiNGAM and is
1884 worst-case: in practice, it took a couple of iterations only in our experiments. Below are the detail
1885 of the derivations for each step of Algorithm 4.

1886 **Computational complexity** The computational complexity of ICA-LiMVAM can be broken
1887 down across the four steps in Algorithm 4. Step 1 calls SharedICA, with its most costly variant
1888 (SharedICA-ML) running in $O(t \cdot n \cdot m \cdot p^3)$, where t is the number of iterations, n the number
1889

1890 of samples, m the number of views, and p the number of components. Step 2 solves the permu-
 1891 tation indeterminacy via a linear sum assignment in $O(m \cdot p^3)$, instead of trying $p!$ permutations.
 1892 Step 3 involves m multiplications with permutation matrices and additions, costing $O(mp^2)$. Step
 1893 4 optimizes over permutations. Instead of trying $p!$ permutations, we use the heuristic Algorithm C
 1894 from LiNGAM. It is $O(m \cdot p^5)$ in the worst case (and much lower in practice). Further details are
 1895 provided next:

- 1896 1. Run the ICA algorithm SharedICA-ML, $O(tnmp^3)$
 1897 Each of the t iterations of the optimization performs the so-called ‘‘E-step’’ and ‘‘M-step’’
 1898 of the E-M algorithm, detailed in Section 4 of Richard et al. (2021). Their complexity is
 1899 in mnp^3 : the intuition is that for each view m and each sample n require some matrix
 1900 operations (e.g. addition, multiplication, computing gradients and Hessians) all of which
 1901 are dominated by p^3 . So the final complexity is in $O(tnmp^3)$.
 1902
- 1903 2. Solve the permutation-sign indeterminacy, $O(mp^3)$
 1904 Computing the objective can be done in $O(p^2)$. The detail of this is: we begin by computing
 1905 the matrix W which is in $O(mp^2)$, then multiplying it with a permutation matrix which is
 1906 in $O(p^2)$, and finally summing the diagonal elements which is in $O(p)$.
 1907 Finding the correct permutation matrix can be done by solving a linear-sum assignment
 1908 problem; this can be done using the Hungarian algorithm which is in $O(p^3)$.
- 1909 3. Update the entries of a matrix which is in $O(p^2)$.
- 1910 4. Update the entries of a matrix which is in $O(p^2)$.
 1911 Adding the complexities thus far leads to a complexity of $O(mp^2 + p^3)$, which is dominated
 1912 by $O(mp^3)$, for Step 2.
- 1913 5. Compute the causal matrices, $O(mp^2)$
 1914 Each of the m causal matrices requires multiplying a dense matrix with a permutation
 1915 which is in $O(p^2)$ and then adding a matrix which is in $O(p^2)$. The final cost is $O(mp^2)$.
 1916
- 1917 6. Find the causal ordering(s), $O(mp^5)$
 1918 Algorithm B in the original LiNGAM paper finds a row that has all zeros $O(p^2)$, removes
 1919 it, does this p times. Its complexity is in $O(p^3)$.
 1920 Algorithm C in the original LiNGAM paper calls Algorithm B at most $p(p-1)/2 = O(p^2)$
 1921 times, so its final complexity is $O(p^2 p^3) = O(p^5)$.
 1922 When the causal ordering is shared across views: first we compute sum m matrices with
 1923 p^2 entries which is in $O(mp^2)$, and then we use Algorithm C once which is in $O(p^5)$. The
 1924 final complexity is in $O(mp^2 + p^5)$ which is dominated by $O(mp^5)$.
 1925 When the causal ordering is view-dependent: for each of the m views, we use Algorithm
 1926 C which is in $O(p^5)$, so the final complexity is in $O(mp^5)$.

1927
 1928
 1929
 1930
 1931
 1932
 1933
 1934
 1935
 1936
 1937
 1938
 1939
 1940
 1941
 1942
 1943

1944 H EXPERIMENTS

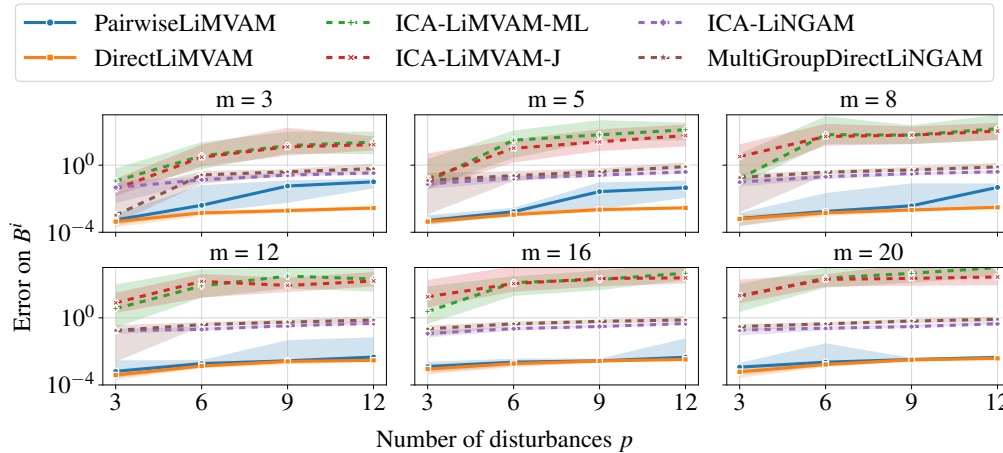
1945 H.1 SYNTHETIC EXPERIMENTS

1946 H.1.1 DATA GENERATION IN FIGURE 1

1947
1948
1949 The causal effect matrices $B^i = P^\top T^i P$ are generated from a random permutation P and strictly
1950 lower triangular T^i obtained from a standard Gaussian; the diagonal matrices D^i are drawn from
1951 a uniform density between 0.1 and 3; the common disturbances in s can be either Gaussian or
1952 non-Gaussian: Gaussian disturbances s_j are generated from a standardized Gaussian and their cor-
1953 responding noises n_j^i have standard deviation Σ_{jj}^i obtained by sampling from a uniform density
1954 between 0 and 1, while non-Gaussian disturbances are generated from a Laplace distribution (with
1955 scale parameter equal to $\frac{1}{2}$) and their corresponding noises all have a std of $\frac{1}{2}$. We use $m = 5$ views,
1956 $p = 4$ variables, and vary the number of samples n between 10^2 and 10^4 .
1957

1958 H.1.2 SIMULATION STUDY IN HIGHER DIMENSION

1959
1960 We evaluate the methods by measuring the estimation error on the matrices B^i across a range of
1961 settings involving more views and components than those considered in the main text. Specifically,
1962 we vary the number of views among $\{3, 5, 8, 12, 16, 20\}$ and the number of components among $\{3,$
1963 $6, 9, 12\}$, using 1000 samples and 50 random seeds for each configuration.
1964



1965
1966
1967
1968
1969
1970
1971
1972
1973
1974
1975
1976
1977
1978
1979
1980 Figure 5: Separation performance of three pairwise-comparisons-based algorithms — Multi-
1981 GroupDirectLiNGAM from Shimizu (2012), and DirectLiMVAM and PairwiseLiMVAM which use
1982 the criteria in Eq. 5 and Eq. 6, respectively — and three ICA-based algorithms — ICA-LiNGAM,
1983 which naively uses Shimizu et al. (2006) separately in each view, and our implementation of the
1984 two variants of ICA-LiMVAM Chen et al. (2024). We varied the number of views and compo-
1985 nents. Disturbances are generated using the generalized normal distribution with shape parameter
1986 $\beta \in \{1.5, 2, 2.5\}$. The metric used is the ℓ_2 -distance between true and estimated causal effect
1987 matrices B^i (lower is better).

1988 Data are generated from the model in Eq. 3, where disturbances e_j are split into three types—sub-
1989 Gaussian, Gaussian, and super-Gaussian—which motivates the choice of disturbance counts as mul-
1990 tiples of 3. Sub-Gaussian disturbances follow a generalized normal distribution with shape param-
1991 eter $\beta = 2.5$; super-Gaussian disturbances use $\beta = 1.5$; Gaussian disturbances correspond to $\beta = 2$.
1992 Each T^i is sampled as a strictly lower-triangular matrix with Gaussian entries, and a common per-
1993 mutation matrix P is used to construct the $B^i = P^\top T^i P$. For each method, we report the median
1994 error on the matrices B^i , with the 25th and 75th percentiles shown as error bars.

1995 As shown in Fig. 5, DirectLiMVAM and PairwiseLiMVAM consistently achieve lower errors than
1996 the other approaches. DirectLiMVAM performs best when the number of views is limited (3, 5,
1997 or 8) while the number of components remains relatively high (9 or 12), thereby outperforming
PairwiseLiMVAM in these settings. This slightly surprising observation that DirectLiNGAM is a

1998
1999
2000
2001
2002
2003
2004
2005
2006
2007
2008
2009
2010
2011
2012
2013
2014
2015
2016
2017
2018
2019
2020
2021
2022
2023
2024
2025
2026
2027
2028
2029
2030
2031
2032
2033
2034
2035
2036
2037
2038
2039
2040
2041
2042
2043
2044
2045
2046
2047
2048
2049
2050
2051

bit better than PairwiseLiNGAM is perhaps due to the fact that there the particular non-Gaussianities used here are ill-suited for the Gaussian likelihood underlying PairwiseLiNGAM.

In contrast, ICA-LiNGAM and MultiGroupDirectLiNGAM achieve slightly better-than-average performance when both the number of views and the number of components are small, but their performance quickly degrades to the average level as dimensionality increases. This behavior reflects their inability to properly handle Gaussian disturbances. Finally, both ICA-LiMVAM variants fail completely, as they are not designed to operate without shared disturbances. Overall, the estimation error tends to increase with the number of components.

H.1.3 COMPARISON WITH A MULTI-DOMAIN METHOD

Here, we illustrate the advantage of using multi-view methods like ours when cross-view correlations are present in the data. Specifically, we compare our DirectLiMVAM to the method of Perry et al. (2022), MSS (see Appendix I). We used their implementation with the KCI estimator, as this variant performs best in their paper. Since MSS recovers only the common DAG structure (and not the causal weights), we measure performance in terms of recovering the causal ordering.

We used the following experimental setup. Data were generated according to Eq. 1 with 6 views, 4 Gaussian disturbances, 500 samples, and the experiment was repeated over 30 random seeds. The noise variances were all fixed to one, and some entries in the matrices B^i were allowed to vary across views. The number of such varying entries corresponds to the number of “interventions”, *i.e.* changes in causal mechanisms in the sense of Perry et al. (2022).

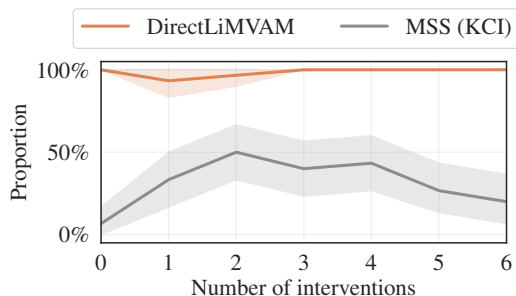


Figure 6: Proportion of runs in which the ordering is perfectly recovered (higher is better). The number of interventions corresponds to the number of entries in the B^i that are allowed to vary across views. We compare our multi-view algorithm DirectLiMVAM to the multi-domain algorithm MSS of Perry et al. (2022) (using the KCI estimator).

Figure 6 shows that DirectLiMVAM always recovers the correct ordering, regardless of how many entries in B^i are allowed to vary. By contrast, MSS fails to recover the DAG when the number of interventions is either too small or too large (in line with their Figures 4 and 5), and even in the regime of sparse interventions it perfectly recovers the ordering in only about 50% of the runs. Finally, their method is substantially slower than ours (not shown in the graph).

These results illustrate the distinction between multi-view and multi-domain methods: by explicitly exploiting cross-view correlations, DirectLiMVAM can achieve stable and accurate recovery in settings where a multi-domain method like MSS fails. Furthermore, this experiment confirms that our methods do not require changes in the B^i as long as there are sufficient correlations between views, thereby extending the identifiability theories in the work just discussed.

H.1.4 TESTING ASSUMPTION 4

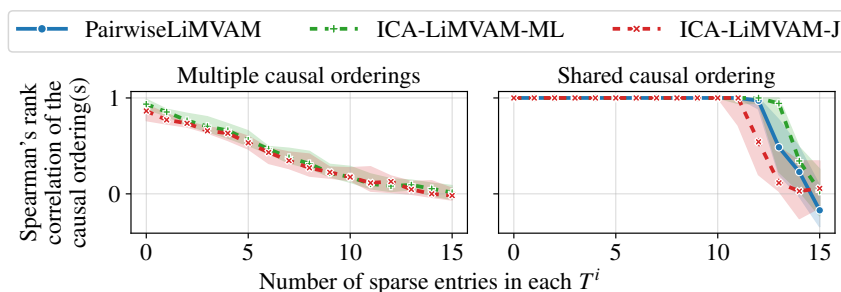
Assumption 4 provides a sufficient condition for the identifiability of the causal matrices B^i in the LiMVAM model with shared, Gaussian disturbances. To evaluate the practical impact of this assumption, we simulated data from the model in Eq. 3, with shared disturbances as in Eq. 9. We used 5 views, 4 common disturbances in s (2 Gaussian and 2 Laplacian), and 1000 samples.

2052 The scale matrices D^i were drawn uniformly
 2053 from the interval $[0.5, 2]$, and the strictly lower
 2054 triangular matrices T^i were sampled from a
 2055 Gaussian distribution and then permuted to
 2056 form the causal matrices B^i . The noise vari-
 2057 ances Σ_{jj}^i corresponding to the Laplacian
 2058 disturbances were fixed to $\frac{1}{2}$, while the noise vari-
 2059 ances corresponding to the two Gaussian
 2060 disturbances, indexed by j and j' , were initially
 2061 sampled uniformly in $[0, 1]$. To test the as-
 2062 sumption, we selected an increasing number
 2063 of views i such that the scaled noise variances
 2064 $\frac{\Sigma_{jj}^i}{D_{jj}^i} = \frac{\Sigma_{j'j'}^i}{D_{j'j'}^i}$, ranging from 0 to 5. Note that
 2065 Assumption 4 only fails when this condition
 2066 holds across all 5 views. We repeated this ex-
 2067 periment over 50 random seeds.

2068 Figure 7 shows that ICA-LiMVAM maintains
 2069 low estimation error on the B^i matrices as long
 2070 as the noise diversity assumption holds, but its
 2071 performance deteriorates sharply once the as-
 2072 sumption is violated. This confirms the practi-
 2073 cal relevance of the assumption. Interestingly, PairwiseLiMVAM appears unaffected by the violation
 2074 of this condition.

2076 H.1.5 TESTING ASSUMPTIONS 5 AND 7

2078 Assumption 5 (resp. Assumption 7) gives a sufficient condition for the identifiability of the causal
 2079 matrix P (resp. causal orderings P^i) and matrices T^i , in the shared causal ordering (resp. multiple
 2080 causal orderings) case. However, it is not straightforward how robust the algorithms are to these
 2081 assumptions.



2093 Figure 8: Spearman's rank correlation between true and estimated causal orderings as a function of
 2094 the number of sparse entries in each T^i . Left: In the multiple-ordering setting, performance of ICA-
 2095 LiMVAM-ML and ICA-LiMVAM-J degrades linearly with increasing sparsity, as the assumption of
 2096 full support is violated. PairwiseLiMVAM is excluded since it assumes a shared ordering. Right: In
 2097 the shared-ordering setting, all methods maintain near-perfect recovery up to 11 sparse entries, after
 2098 which performance drops sharply.

2100 To evaluate the practical impact of these two assumptions, we simulated data from the model
 2101 in Eq. 3, with shared disturbances as in Eq. 9. We used 8 views, 6 common disturbances (two
 2102 sub-Gaussians sampled from a generalized normal distribution with shape parameter $\beta = 2.5$; two
 2103 super-Gaussians for $\beta = 1.5$; two Gaussians corresponding to $\beta = 2$), and 1000 samples. The scale
 2104 matrices D^i were drawn uniformly from the interval $[0.5, 2]$, the strictly lower triangular matrices
 2105 T^i were sampled from a Gaussian distribution and then permuted to form the causal matrices B^i ,
 and the variances Σ^i were sampled uniformly in $[0, 1]$. The experiment was repeated 30 times.

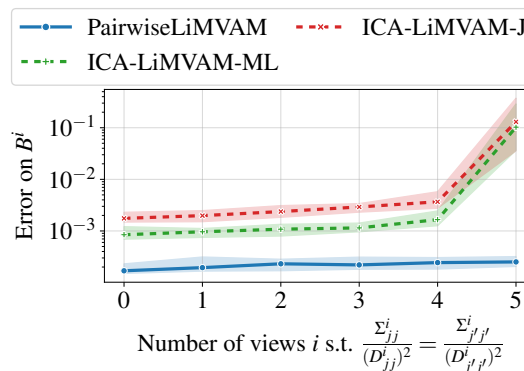


Figure 7: Effect of violating the noise diversity assumption (Assumption 4) on the estimation error of the causal matrices B^i . We report the average ℓ_2 error over 50 repetitions for ICA-LiMVAM and PairwiseLiMVAM, as the number of views with identical scaled noise variances increases.

2106 Fig. 8 reports the Spearman’s rank correlation between the true and estimated causal orderings as
 2107 a function of the number of sparse entries in each T^i , randomly chosen among the $6 \times 5 = 30$
 2108 non-zero entries.

2109 In the multiple causal orderings setting (left panel), both ICA-LiMVAM variants exhibit a roughly
 2110 linear drop in performance as sparsity increases. This behavior is expected, as Assumption 7 no
 2111 longer holds once any entry in the strictly lower triangular part of T^i is set to zero. Pairwise-
 2112 LiMVAM is not included in this setting, as it is designed under the assumption of a shared causal
 2113 ordering.

2114 In the shared causal ordering setting (right panel), all methods benefit from the shared structure
 2115 and recover the true ordering P reliably up to 11 sparse entries. Beyond this point, performance
 2116 degrades sharply for all methods, reflecting the increasing violation of Assumption 5.

2117 These results empirically support the practical relevance of Assumptions 5 and 7.

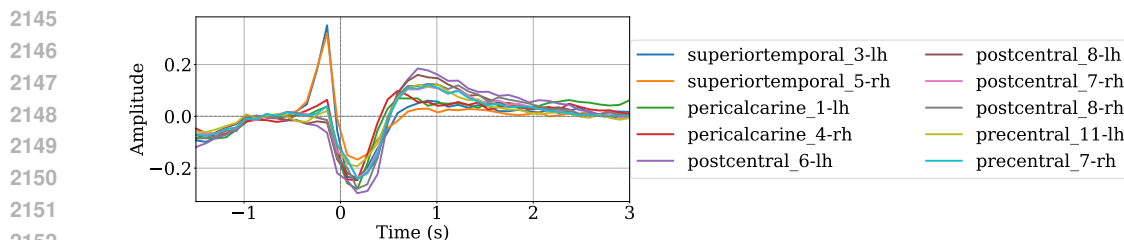
2120 H.2 REAL DATA EXPERIMENTS

2122 H.2.1 DETAILS ON THE PREPROCESSING OF MEG DATA

2123 The MEG data measures participants’ responses to auditory and visual stimuli. The auditory stimuli
 2124 were binaural pure tones. The visual stimuli were checkerboards presented both to the left and right
 2125 of a central fixation for 34-ms duration. This task leads to strong signal power modulations during
 2126 the motor preparation and motor execution.

2127 The original MEG data were acquired with 306 sensors, recorded at 1000 Hz, and band-pass filtered
 2128 between 0.03 and 330 Hz. All MEG processing was done using the MNE-Python library (Gramfort
 2129 et al., 2013; 2014) and we largely followed the pre-processing steps used in Power et al. (2023). We
 2130 applied a Maxwell filter Taulu & Simola (2006) to improve data quality and a band-pass filter be-
 2131 tween 8 and 27 Hz to focus on power effects spread over the alpha and beta bands of the brain. This
 2132 range of waves is supposed to be particularly active in sensorimotor tasks, especially during move-
 2133 ment preparation and execution, and it typically shows a characteristic suppression (event-related
 2134 desynchronization) during movement, followed by a rebound (event-related synchronization) after
 2135 movement cessation, which is thought to reflect sensorimotor processing and inhibitory mecha-
 2136 nisms. In particular, the suppression and rebound are reflected in the energies of the signals, not raw
 2137 signals.

2138 The data were then parsed into trials synchronized to each button press, with a duration of 4.5 s,
 2139 including a 1.5 s pre-movement interval. The 4.5 s window length was selected to ensure a sufficient
 2140 post-movement interval to capture the entire beta rebound response. Trials were excluded if the
 2141 button press occurred more than 1 s after the audiovisual cue (indicating poor task performance) or
 2142 if another button press occurred within the time window. Then, a baseline correction was applied
 2143 using the pre-movement interval (-1.5 s, -1 s). The procedure led to about 60 trials per participant
 2144 on average.



2153 Figure 9: Example of time series obtained after the preprocessing. We averaged the data across
 2154 subjects and trials, resulting in 10 time series, one for each brain region.

2155 Next, we performed a cortical projection. First, each participant’s MRI (additionally given in the
 2156 Cam-CAN database) was segmented using FreeSurfer Dale et al. (1999). The segmentation provided
 2157 a digitization of the cortical surface for source estimation, a transformation to the average brain (*i.e.*
 2158 fsaverage) for spatial normalization and group statistics, and a boundary element model of the head
 2159 to provide more accurate calculation of the forward solution. The inverse solution, based on the

2160 MNE method Hämäläinen & Ilmoniemi (1994), allowed to consider cortical region activations for
2161 further analysis.

2162 We used the cortical parcellation from Khan et al. (2018) to divide the
2163 cortical mantle (both hemispheres) into 448 distinct regions and summa-
2164 rized each region by an averaged time course. Then, we selected 10 of
2165 the 448 regions based on their known importance in sensorimotor tasks.
2166 Specifically, we picked for each hemisphere three regions in the motor
2167 cortex (two parcels in the “postcentral” and one in the “precentral”; vis-
2168 ible in blue in Fig. 3a), one region in the auditory cortex (“superiortem-
2169 poral” parcel; highlighted in pink), and one region in the visual cortex
2170 (“pericalcarine” parcel; not visible in the figure). Note again that the task
2171 for the participant is active as right index button presses are triggered by
2172 audiovisual stimulations.

2173 For each participant, we thus extracted one time series for each of the 10
2174 regions and fixed the number of trials to 40. Participants with less than
2175 40 trials were discarded and extra trials were averaged. Participants for
2176 whom some of the parcels did not have any vertex in the source space
2177 were also discarded, resulting in a total of 98 available participants. We
2178 performed a Z-score normalization of the time series to correct the depth
2179 bias and, importantly, computed the Hilbert *envelope* of the signals to
2180 study modulations in cortical source power. Finally, the signals were centered and downsampled
2181 from 1000 Hz to 10 Hz due to the slowly changing nature of the envelopes (energies). The final
2182 dataset consisted of 98 subjects, 10 brain regions, and 1760 time points.

2183 Figure 9 shows the typical time series obtained after preprocessing. For visualization, we averaged
2184 the time courses across participants and trials. As expected, we observe a prominent peak in the
2185 “superiortemporal” auditory regions shortly before the button press ($t = 0$ s), reflecting the stimulus
2186 onset. In the motor regions, a characteristic rebound pattern emerges: the signals decrease around
2187 the time of the button press, consistent with event-related desynchronization of beta rhythms, and
2188 subsequently increase after approximately 0.3 seconds, indicating beta resynchronization. This fig-
2189 ure also labels the ten cortical parcels selected for analysis.

2190 H.2.2 MEG EXPERIMENT USING ICA-LiMVAM-ML

2191 In the following, we present additional analyses that extend the experiments described in Section 6.2.

2192 Figure 11 displays median causal effect maps estimated using ICA-LiMVAM-ML on the Cam-CAN
2193 dataset. For each of the six panels, ICA-LiMVAM-ML was applied to a randomly chosen subset of
2194 50% of the participants. These results are consistent with the patterns observed in Figure 3a, notably
2195 the frequent presence of directed connections between motor areas in opposite hemispheres. This
2196 further supports the hypothesis of consistent inter-hemispheric causal influences in sensorimotor
2197 processing.

2198 Finally, we conducted the same robustness analysis for ICA-LiMVAM-ML as previously done for
2199 PairwiseLiMVAM (Figure 3b). Specifically, we ran ICA-LiMVAM-ML 50 times, each time using a
2200 randomly selected subset of 30 participants from the full cohort, and computed the Pearson corre-
2201 lations between the element-wise median of the estimated individual matrices B^i across runs. The
2202 resulting correlations are shown in Figure 10. While the correlations remain predominantly positive
2203 (with an average of 0.27), they are noticeably lower than those obtained with PairwiseLiMVAM.
2204 This suggests that, in terms of stability across subsets, PairwiseLiMVAM exhibits greater consis-
2205 tency than ICA-LiMVAM-ML.

2206
2207
2208
2209
2210
2211
2212
2213

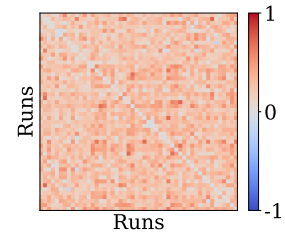


Figure 10: Pearson correlations between median causal effect matrices across 50 runs of ICA-LiMVAM-ML, each using a different random subset of 30 participants from the Cam-CAN cohort.

2214
2215
2216
2217
2218
2219
2220
2221
2222
2223
2224
2225
2226
2227
2228
2229
2230
2231
2232
2233
2234
2235
2236
2237
2238
2239
2240
2241
2242
2243
2244
2245
2246
2247
2248
2249
2250
2251
2252
2253
2254
2255
2256
2257
2258
2259
2260
2261
2262
2263
2264
2265
2266
2267

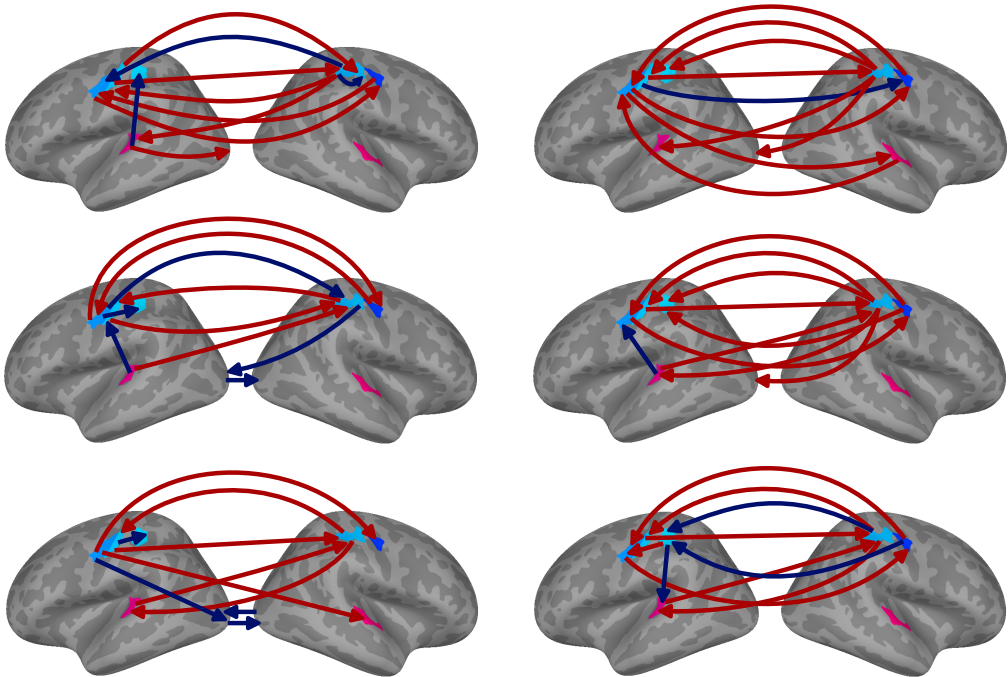


Figure 11: Top ten strongest median causal effects (estimated by ICA-LiMVAM-ML) of six different runs. Each run was performed on the data of 49 randomly chosen subjects. Red arrows represent positive effects and blue arrows negative effects.

2268
2269
2270
2271
2272
2273
2274
2275
2276
2277
2278
2279
2280
2281
2282
2283
2284
2285
2286
2287
2288
2289
2290
2291
2292
2293
2294
2295
2296
2297
2298
2299
2300
2301
2302
2303
2304
2305
2306
2307
2308
2309
2310
2311
2312
2313
2314
2315
2316
2317
2318
2319
2320
2321

I DISTINCTION BETWEEN MULTI-VIEW AND MULTI-DOMAIN FRAMEWORKS

Several frameworks study causal discovery from multiple related datasets that share the same causal structure. While *multi-view* methods (like ours) model *correlated* views arising from a joint (non-factorial) distribution, *multi-domain* methods treat datasets as *independent* domains drawn from related but distinct distributions. Consequently, multi-domain methods cannot leverage cross-view correlations and instead rely exclusively on distributional shifts across domains. *Multi-environment* methods are a special case of multi-domain methods, where distributional shifts arise from *interventions* (whether designed by the practitioner or arising from uncontrolled environment differences) on the causal mechanisms. In the following, we review some multi-domain/multi-environment methods that are related to our work.

Ghassami et al. (2018) propose a multi-domain method that, like ours, studies linear causal discovery from multiple datasets that share the same underlying DAG in the causally sufficient setting and without a non-Gaussianity assumption. However, they assume that causal mechanisms $\mathbb{P}(x_j^i | \mathbf{PA}_j^i)$ are *independent* (both within and across domains), where \mathbf{PA}_j^i denotes the parents of x_j^i . Our approach does not require such an independence assumption. For identifiability of the true DAG, their method further assumes that noise variances or causal weights vary across domains, and one of their two criteria additionally requires these changes to be sparse. In our paper, we show that such changes in noise variances are sufficient for identifiability (see Assumption 6), but not necessary when the views exhibit diverse correlations.

Adams et al. (2021) study multi-domain identifiability in the more complex setting of *latent confounders*. Their main contributions are necessary and sufficient conditions (bottleneck and strong non-redundancies) that are specific to the confounded setting and vanish in our causally sufficient case. In particular, in this causally sufficient case, their conditions reduce to assuming heterogeneous variances (see their Theorem 1), which is precisely one of the sufficient conditions in our Assumption 6. Moreover, they require the causal weights \mathbf{B}^i to *remain constant* across domains, which is a strong assumption we do not make. Thus, in the causally sufficient case, our method encompasses theirs and goes much further by leveraging correlations (across views and within a view), while allowing causal weights to differ. They suggested, in fact, that their assumptions were too strong in Section 3: “Note that this theorem gives sufficient conditions; our empirical results suggest that they are not necessary.”

Peters et al. (2016) propose a multi-environment method that aims to identify the parents of a *single target variable* rather than recovering the full graph, while assuming purely *Gaussian* distributions. Their approach relies on *invariance* of the target’s causal mechanism across environments, which implicitly requires knowing where interventions occurred (and that the target was not intervened upon), an assumption that is often unrealistic in practice.

Similarly, Perry et al. (2022) propose another multi-environment method that leverages invariance and can be more easily applied to causal discovery of the whole structure. However, their method considers the more complex case of *nonlinear* relationships. Like Ghassami et al. (2018), they rely on changes in $\mathbb{P}(x_j^i | \mathbf{PA}_j^i)$ across environments, but instead of measuring independence between mechanisms, they count how often these mechanisms change and select the DAG that minimizes this number. Their identifiability results require sparsity in the number of changes; in particular, not all causal mechanisms are allowed to differ across environments. In contrast, our theory accommodates arbitrarily many changes in \mathbf{B}^i and in the distribution of e^i ; moreover, these changes are not required for identifiability if cross-view correlations are diverse.